Table 1
The accession numbers of TLRs and innate immunity genes used for BLAST and phylogenetic analyses. The accession numbers of NCBI are listed. Only *X. tropicalis* TLRs are indicated by JGI ID.

Species	Gene name			
Homo sapiens	TLR1 (U88540)	TLR2 (U88878)	TLR3 (U88879)	TLR4 (U88880)
	TLR5 (NM_003268)	TLR6 (NM_006068)	TLR7 (NM_016562)	TLR8 (NM_016610)
	TLR9 (AF259262)	TLR10 (AF296673)	MyD88 (NP_002459.1)	TICAM-1 (AB086380)
	TICAM-2 (NP_067681.1)	TIRAP (NP_001034750.1)	SARM (NP_055892.2)	LBP (NP_004130.2)
	CD14 (NP_001035110.1)	MD2 (NP_056179.2)	RIG-I (AF038963)	MDA5 (AF095844)
	LGP2 (NP_077024.2)	IPS-1 (NP_065797.2)	IRAK1 (NM_001025242)	IRAK2 (NM_001025242)
	IRAK3 (NP_001135995.1)	IRAK4 (NM_001114182)	TRAF3 (NM_003300)	TRAF6 (NM_004620)
	TAB2 (NM_015093)	TAB3 (NM_152787)	TBK1 (NP_037386.1)	RIP1 (NP_003795)
	CASP8 (NP_001219.2)	FADD (NP_003815.1)	TANK (NP_004171.2)	SINTBAD (NP_055541.1)
	IKKα (NP_001269.3)	IKKβ (NP_001547.1)	IKKγ (NP_001093327.1)	IKKε (NP_054721.1)
	NAP1 (NP_071906.1)	MKK6 (NP_002749.2)	MKK3 (NP_002747.2)	JNK (NP_002741)
	TAB2 (NM_015093)	IRF3 (NP_001562.1)	IRF7 (NP_001563.2)	RELA (NP_001138610.1)
	NFκB1 (NP_001158884.1)	ATF2 (NP_001871.2)	AP-1 (NP_034721.1)	Mx (NM_001144925)
	PKR (NM_001135651)	OAS1 (NM_001032409)	IFNα (NM_024013)	IFNβ (NM_002176)
	TNFα (NP_000585)	IL-6 (NM_000600)	IL-12p40 (NP_002178.2)	
M. musculus	TLR1 (NM_030682)	TLR2 (NM_011905.3)	TLR3 (NM_126166)	TLR4 (NM_021297)
	TLR5 (NM_016928)	TLR6 (NM_011604)	TLR7 (NM_133211)	TLR8 (NM_133212)
	TLR9 (NM_031178)	TLR11 (NM_205819)	TLR12 (NM_205823)	TLR13 (NM_205820)
	MyD88 (NP_034981.1)	TICAM-1 (NP_778154.1)	TICAM-2 (NP_775570.1)	TIRAP (NP_473437.1)
	SARM (NP_766383.2)			
G. gallus	TLR1 (NM_001007488)	TLR2 (NM_204278)	TLR3 (NM_001011691)	TLR4 (NM_001030693)
	TLR5 (NM_001024586)	TLR6 (NM_001007488)	TLR7 (NM_001011688)	TLR15 (NM_001037835)
	TLR21 (NM_001030558)	MyD88 (NP_001026133.1)	TICAM-1 (NM_001081506)	TIRAP (NP_001020000.1)
	SARM (XP_415814.2)			
X. tropicalis	TLR1 (jgi371271)	TLR2.1 (jgi320872)	TLR2.2 (jgi320954)	TLR3 (jgi271893)
	TLR5 (jgi459490)	TLR6.1 (jgi281677)	TLR6.2 (jgi371307)	TLR7 (jgi323633)
	TLR8.1 (jgi161716)	TLR8.2 (jgi323721)	TLR9 (jgi350411)	TLR12 (jgi187046)
	TLR14.1 (jgi190020)	TLR14.2 (jgi30694)	TLR14.3 (jgi421728)	TLR14.4 (jgi421736)
	TLR21 (jgi349648)	TLR22 (jgi414791)	MyD88 (DR867184)	TICAM-1 (CX999107.1)
	TIRAP (NM_001044460)			
D. rerio	TLR1 (XM_692439)	TLR2 (NM_212812.1)	TLR3 (AY616582)	TLR4a (NM_001131051)
	TLR4b (NM_212813)	TLR5a (XP_001919052)	TLR5b (XM_001343113)	TLR7 (XP_701101.3)
	TLR8a (XP_001920594)	TLR8b (XM_001340150)	TLR9 (XM_685911)	TLR12 (XM_685162)
	TLR14 (NM_001089350)	TLR18(BC162732)	TLR21 (XP_001923227.1)	TLR22 (XM_692565)
	MyD88 (NP_997979.2)	TICAM-1 (NP_001038224.1)	TIRAP (XP_001922965.1)	SARM (XP_001344407.1)
T. rubripes	TLR1 (AAW69368)	TLR2 (AAW69370)	TLR3 (AC156436)	TLR5 (AC156437)
	TLR5S (AC156440)	TLR7 (AC156438)	TLR8 (AC156438)	TLR9 (AC156439)
	TLR14 (AC156431)	TLR21 (NM_001032579)	TLR22 (NM_001113193)	TLR23 (AC156435)
	MyD88 (NM_001113195)	TICAM-1(NM_001113194)	TIRAP (NM_001113196)	
Lethentron japonicum	TLR14a (AB109402)	TLR14b (AB109403)		

(pmTLRs) (Fig. 1). The other 4 proteins were defined as TLR adaptor-like proteins since they are similar to MyD88, TICAM or SARM.

Based on the Genscan ID and EST accession numbers, the contig positions and *E*-values for the 16 pmTLR proteins were determined, and each protein was annotated based on their most likely TLR homolog (Table 2). Sea lamprey pmTLR14a and pmTLR14b were most homologous to Japanese lamprey laTLR14a (ljTLR14a) and laTLR14b (ljTLR14b), respectively, which we previously identified (Ishii et al., 2007b). An additional two genes, pmTLR14c and pmTLR14d, encoded paralogs of ljTLR14a and b, and were more homologous to zebrafish TLR18 than any other TLR family member. Additionally, we found four TLR2-like genes formed a unique cluster independent of the clade of the mammalian TLR2 (Fig. 2). Therefore, we designated these pmTLR genes TLR24a-d, which represent a novel TLR2 subfamily. TLR2c and d both localized to contig 1344, suggesting a cause of gene duplication, however, the presence of an ambiguous gap between the two genes deterred us from concluding that they originated from a tandem duplication. It is notable that the TLR7/8, TLR14, and TLR21 genes were mapped to distinct contigs. Although pmTLR2c appeared to be an ortholog of *Canis lupus* TLR6, its functional similarity to mammalian TLR6 could not be determined. Lamprey possessed orthologous genes for TLR3, TLR5, TLR7, and TLR8 but not for TLR4 or TLR9. In addition to the M-type TLRs, three TLR21 and a single TLR22 orthologs classified as F-type TLRs were identified in the lamprey genome database. Taken together, the phylogenetic analyses revealed that sea lamprey has a TLR system comprised of an incomplete set of M-type and full F-type TLRs, as in fish (Fig. 1).

Although many animal TLR genes are predicted to be intronless (Roach et al., 2005), *T. rubripes* TLR genes have been reported to contain introns and be dispersed over wide regions on a variety of chromosomes (Oshiumi et al., 2003a). In the Pre-Ensemble Lamprey Genome database, lamprey TLR2d, 3, 14c, 22, and 24d contain several introns in coding regions, while TLR2a, 2b, 14a, 14b, 21a, 21b, 21c, 24a and 24b are intronless. As only partial sequences for TLR2c, 5, 7, 8a, 8b, 14d, and 24c were obtained from the genome database, it was impossible to conclusively determine if introns were present. Nevertheless, the results infer that lamprey TLRs are encoded by both intron-containing and intronless genes, as is the case in teleosts (Oshiumi et al., 2003a).

Using the SMART program, typical TLR structures of pmTLR proteins were predicted (Fig. 1). Almost all proteins consisted of multiple LRRs in the N-terminal region and a single TIR domain in the C-terminus, split by a transmembrane domain. Although we failed to detect the N- or C-terminal regions in several pmTLRs, their mRNAs, except for TLR24c, were detected by RT-PCR, suggesting that the mRNAs of these pmTLRs are present as complete forms but their signal peptides and N-terminal LRRs could not be

Please cite this article in press as: Kasamatsu, J., et al., Phylogenetic and expression analysis of lamprey toll-like receptors. Dev Comp Immunol (2010), doi:10.1016/j.dci.2010.03.004

Table 2
Annotation of TLR and other innate immunity genes in the *P. marinus* genome. Each TLR and other innate immune gene was annotated using a BLASTP search and described as a TLR after meeting specific criteria. The encoded contig numbers and *E*-value are shown.

Gene categories	Gene name (*P. marinus*)	Genscan prediction ID or EST accession no.	Contig no.	Most similar gene [species] (accession no.)	*E*-value
TLR and their adaptor genes	TLR2a	GENSCAN00000027249	7641	Toll-like receptor 2 [*Sus scrofa*] (BAD90590)	2e-108
	TLR2b	GENSCAN00000120185	1179	TLR2 type2 [*G. gallus*] (BAB16842)	3e-121
	TLR2c	GENSCAN00000113984	1344	Toll-like receptor 6 [*Canis lupus familiaris*] (ACB41375)	2e-83
	TLR2d	GENSCAN00000096816	1344	Toll-like receptor b [*L. japonicum*] (BAE47506)	4e-50
	TLR14a	GENSCAN00000120396	35588	Toll-like receptor a [*L. japonicum*] (BAE47505)	0.0
	TLR14b	EB082826	4136	Toll-like receptor b [*L. japonicum*] (BAE47506)	0.0
	TLR14c	GENSCAN00000075432	9099	Toll-like receptor a [*L. japonicum*] (BAE47505)	7e-170
	TLR14d	GENSCAN00000133414	47492	Toll-like receptor 18 [*D. rerio*] (AAI62732)	2e-135
	TLR3	GENSCAN00000116058	18297	Toll-like receptor 3 [*Taeniopygia guttata*] (XP_002190888)	3e-134
	TLR5	GENSCAN00000136769	38231	TLRS5 [*T. rubripes*] (AAW69378)	4e-87
	TLR7/8a	GENSCAN00000159232	7539	Toll-like receptor 7 [*T. guttata*] (XP_002194911)	0.0
	TLR7/8b	Not predicted	30480	Similar to TLR8 [*Ornithorhynchus anatinus*] (XP_001515241)	2e-122
	TLR21a	GENSCAN00000145839	1528	Toll-like receptor 21 [*Ictalurus punctatus*] (ABF74622)	8e-175
	TLR21b	GENSCAN00000112026	15848	Toll-like receptor 21 [*I. punctatus*] (ABF74622)	2e-154
	TLR21c	GENSCAN00000006564	16741	Toll-like receptor 21 [*D. rerio*] (CAQ13807)	8e-146
	TLR22	GENSCAN00000052970	44660	Toll-like-receptor [*Oncorhynchus mykiss*] (CAF31506)	5e-92
	MyD88	gnl|ti|1309469868	8673	Similar to MyD88 [*Canis familiaris*] (XP_534223)	5e-47
	TICAM-1.1	GENSCAN00000029725	3393	Similar to TICAM-1 [*Monodelphis domestica*] (XP_001375102)	1e-27
	TICAM-1.2	GENSCAN00000011455	28649	TIR-containing adaptor molecule [*I. punctatus*] (ABD93874)	4e-22
	SARM	EC383618	12108	Sterile alpha and TIR motif containing 1 [*D. rerio*] (AAI63770)	2e-95
RLR and adaptor genes	RIG-I	CO546225	50584	RIG-I isoform 1 [*Pan troglodytes*] (XP_001156442)	5e-36
	LGP2	GENSCAN00000019608	2627	DHX58 [*Salmo salar*] (NP_001133649.1)	2e-13
	IPS-1	FD727562	427	Zgc:158392 [*D. rerio*] (AAI29222)	6e-11
TLR/RLR associated genes	LBP	DW024367	9431	MGC108117 protein [*X. tropicalis*] (NP_001015694.1)	2e-42
	IRAK1	GENSCAN00000011724	14150	IRAK1 protein [*Bos taurus*] (AAI08133.1)	5e-25
	IRAK3	GENSCAN00000072175	17420	novel protein similar to vertebrate IRAK3 [*D. rerio*] (CAQ13227.1)	1e-15
	IRAK4	FD717813	6289	IRAK4 [*Plecoglossus altivelis altivelis*] (BAH58736.1)	1e-22
	TRAF3	FD703125	45178	TRAF3 [*O. mykiss*] (NP_001118087.1)	1e-50
	TRAF6	GENSCAN00000012099	4693	TNF receptor-associated factor 6 [*Sus scrofa*] (NP_001098756.1)	3e-134
	TAK1	FD720776	2510	MAP kinase 7 [*X. tropicalis*] (NP_001093731.1)	2e-84
	TAB2	GENSCAN00000012731	19927	Similar to KIAA0733 [*M. domestica*] (XP_001370832.1)	7e-26
	TBK1	EB718759	13265	TANK-binding kinase 1 [*X. tropicalis*] (NP_001135652.1)	2e-21
	RIP1	gnl|ti|1229574012	1789	RIP1 [*Rattus norvegicus*] (NP_001100820.1)	5e-33
	CASP8	EG023282	11270	Caspase 8 [*G. gallus*] (NP_989923)	4e-14
	IKKα	GENSCAN00000034882	5202	IKKα [*T. guttata*] (XP_002186613.1)	3e-60
	IKKβ	GENSCAN00000073839	4708	Unnamed protein product [*Tetraodon nigroviridis*] (CAG09394.1)	3e-12
	IKKγ	CO548529	49136	Similar to IKKγ [*O. anatinus*] (XP_001505706.1)	5e-40
	IKKε	GENSCAN00000078948	48353	IKKε [*B. taurus*] (NP_001039810.1)	8e-16
	NAP1	GENSCAN00000070143	780	5-azacytidine induced 2 [*B. taurus*] (NP_001070473.1)	6e-13
	MKK6	GENSCAN00000036211	17299	Unnamed protein product [*T. nigroviridis*] (CAG03047.1)	2e-14
Transcription factor genes	IRF2	GENSCAN00000117845	17476	Similar to IRF2 isoform 1 [*Canis familiaris*] (XP_532847.2)	8e-47
	IRF4	GENSCAN00000134889	77775	Interferon regulatory factor 4 [*Equus caballus*] (XP_001487915.1)	6e-23
	IRF5	GENSCAN00000119547	65651	unnamed protein product [*T. nigroviridis*] (CAF90666.1)	2e-12
	IRF8	gnl|ti|1220653061	74379	Interferon regulatory factor 8 [*D. rerio*] (NP_001002622.1)	1e-11
	RELA	GENSCAN00000045445	69770	RELA isoform 1 [*H. sapiens*] (NP_068810.3)	3e-15
	NFκB1	CO548333	23299	Similar to NFκB1 p105 subunit [*D. rerio*] (XP_001339487.2)	1e-49
	ATF2	gnl|ti|1229751035	1160	Similar to ATF2 [*M. domestica*] (XP_001376719.1)	6e-09
	AP-1	GENSCAN00000027406	61254	unnamed protein product [*Coturnix coturnix*] (CAA33553.1)	2e-32
Antiviral genes	Mx	EE737404	23777	Mx protein [*Ctenopharyngodon idella*] (Q6TKS7)	2e-11
Not found	TLR4, TLR9, TLR13, TLR15, CD14, MD2, TIRAP, MDA5 IRAK2, TAB3, FADD, TANK, SINTBAD, MKK3, PKR, OAS1, Type I IFN (IFNα, β), TNF-α, IL-6, IL-12p40				

detected in the SMART browser. The size and number of the LRRs in each pmTLR were similar to the TLR counterparts of *T. rubripes* (Fig. 1).

3.2. Phylogenetic analysis of TLRs

To examine the relationships between vertebrate (human, mouse, chicken, xenopus, zebrafish, fugu, and lamprey) TLRs, a phylogenetic tree was constructed based upon the TLR sequences using the Clustal X and MEGA programs (Fig. 2). Phylogenetic analyses, which included the cytoplasmic TIR and extracellular LRR-regions, were performed as described previously (Ishii et al., 2007b). The constructed tree revealed the presence of several TLR subfamilies in pmTLRs: single clades were formed with TLR2a-b, TLR14a-c, TLR7/8a-b, TLR21a-c, and TLR24a-b. It is possible that each subfamily diverged through gene duplications that occurred after lampreys separated from the ancestor of common vertebrates.

There appeared to be a distinct cluster of pmTLR24, which formed a distinct clade from TLR2 and TLR1, 6, 10 in jawed vertebrates and the TLR14 subfamily. It is likely that the lamprey TLR2 subfamily expanded in a lamprey-specific manner. TLR14d was identified as an ortholog of TLR14 of jawed vertebrates with a high bootstrap value, forming a clade with the teleost TLR14 subfamily. In contrast, pmTLR14a-c showed a high similarity to ljTLR14a/b as indicated by their bootstrap values, suggesting that lamprey has two types of TLR14 with different primary sequences.

Although both pmTLR7/8a and 7/8b were mapped to the TLR7/8 cluster of jawed vertebrates, they separated in lamprey species independently of the divergence of TLR7 and TLR8 in jawed vertebrates. Whether pmTLR7/8a and 7/8b recognize nucleic acid

Please cite this article in press as: Kasamatsu, J., et al., Phylogenetic and expression analysis of lamprey toll-like receptors. Dev Comp Immunol (2010), doi:10.1016/j.dci.2010.03.004

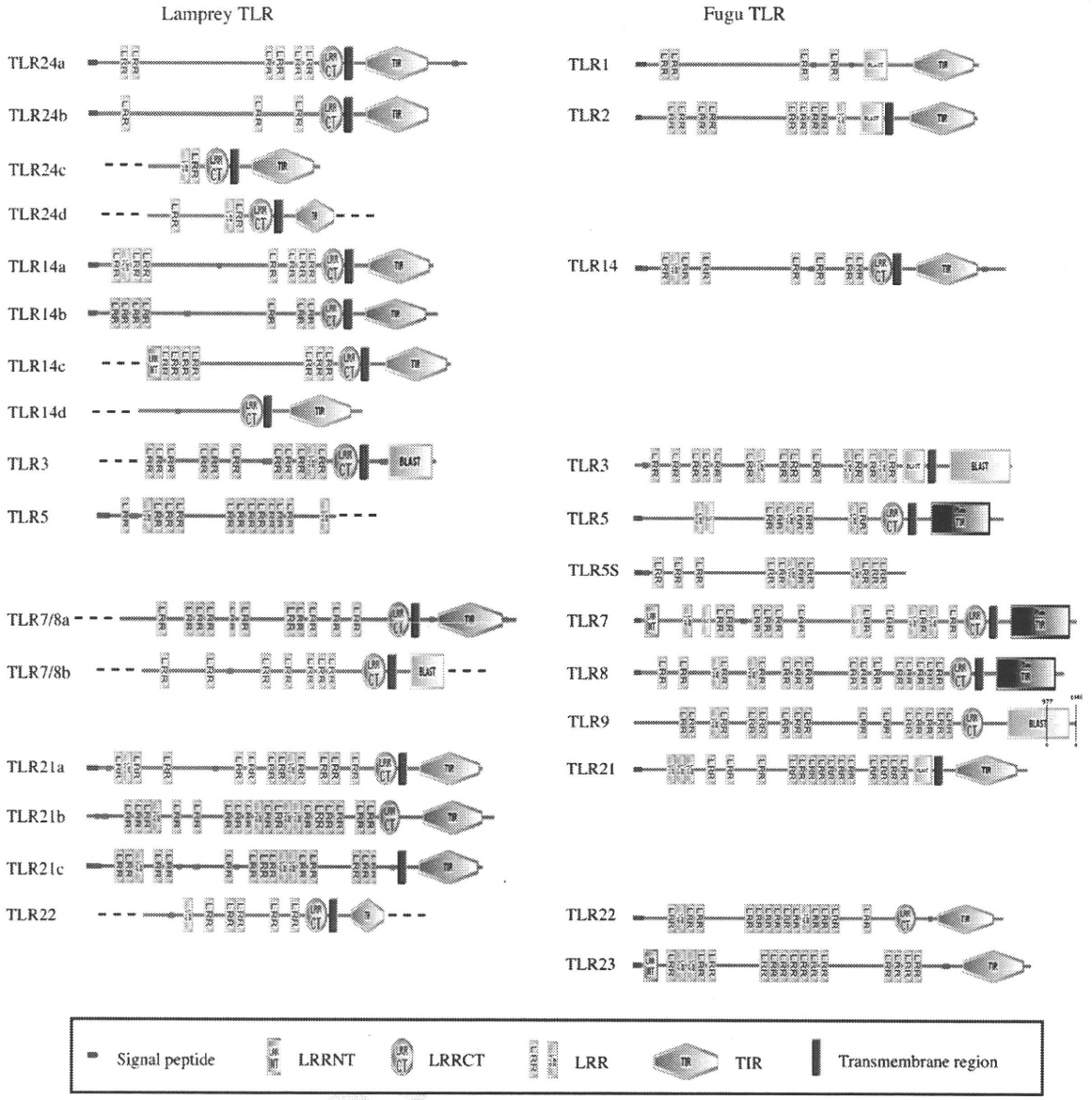

Fig. 1. Structures of the predicted *P. marinus* TLR proteins. Domains in the protein were predicted by the SMART program. LRRNTLRR, LRRCT transmembrane region and TIR domains are indicated in the picture. Left; lamprey TLRs. Right; fugu (*T. rubripes*) TLRs.

structures with different properties is presently unknown. The pmTLR21a-c genes were in the same cluster as the teleost TLR21 clade, while pmTLR22 was closest to the teleost TLR22 gene. There are only a single orthologs of TLR3 and TLR5 in lamprey (Fig. 2), which is consistent with a previous report on vertebrate TLR phylogenetic analysis (Kasahara, 2007). An examination of the tree suggests a rationale that lamprey TLRs correspond to the jawed vertebrate TLR orthologs (Fig. 2). The loci of these genes did not suggest that gene duplications simply occurred in the region resulting in two tandem sets of pmTLR14 and pmTLR24; the splitting of tandem genes may have occurred during the long history of the lamprey. The phylogenetic analysis based on their amino acid sequences reinforced the differential clustering of these TLR clades, which was likely rooted in the 'TLR big-bomb' which occurred ~600 million years ago (Ishii et al., 2007a).

3.3. Phylogenetic analyses of lamprey TLR adaptors

Human and mouse TLRs recruit the TIR-containing adaptors, MyD88 and TICAM-1 (Liew et al., 2005). For example, TLR2 recruits the complex adaptor TIRAP-MyD88, while TLR4 recruits two complex adaptors: TIRAP-MyD88 and TICAM-2–TICAM-1 (Takeda et al., 2003; Liew et al., 2005). The MyD88 pathway is dominant in mammals given that all TLRs, except for TLR3, bind MyD88. Only TLR3 and TLR4 link to the TICAM-1 pathway (Oshiumi et al., 2003b). The present lamprey TLR adaptor analyses allowed us to identify two TICAM-1 homologs, pmTICAM-1a and pmTICAM-1b (Fig. 3(A)), which resemble zebrafish TICAM-1, lacking the TRAF6-binding motif (Sullivan et al., 2007). The RHIM-like domain was conserved in pmTICAM-1b, as in zebrafish TICAM-1, but not in TICAM-1a. In the phylogenetic tree, pmTICAM-1a and b formed a clade with jawed vertebrates as well as mammalian TICAM-1 and 2 with high bootstrap values (Fig. 3(B)). In contrast, pmMyD88 and pmSARM belongs to their respective clades to form a single cluster with MyD88 and SARM of other jawed species with a high bootstrap support (Fig. 3(B)). From the observed amino acid identities between lamprey and jawed vertebrate TICAM genes, pmTICAM-1b was more similar to jawed vertebrate TICAM-1 than to TICAM-2, although pmTICAM-1a was nearly equidistant from all TICAM genes (Table 4). Therefore, these analyses indicate that pmTICAM-

Please cite this article in press as: Kasamatsu, J., et al., Phylogenetic and expression analysis of lamprey toll-like receptors. Dev Comp Immunol (2010), doi:10.1016/j.dci.2010.03.004

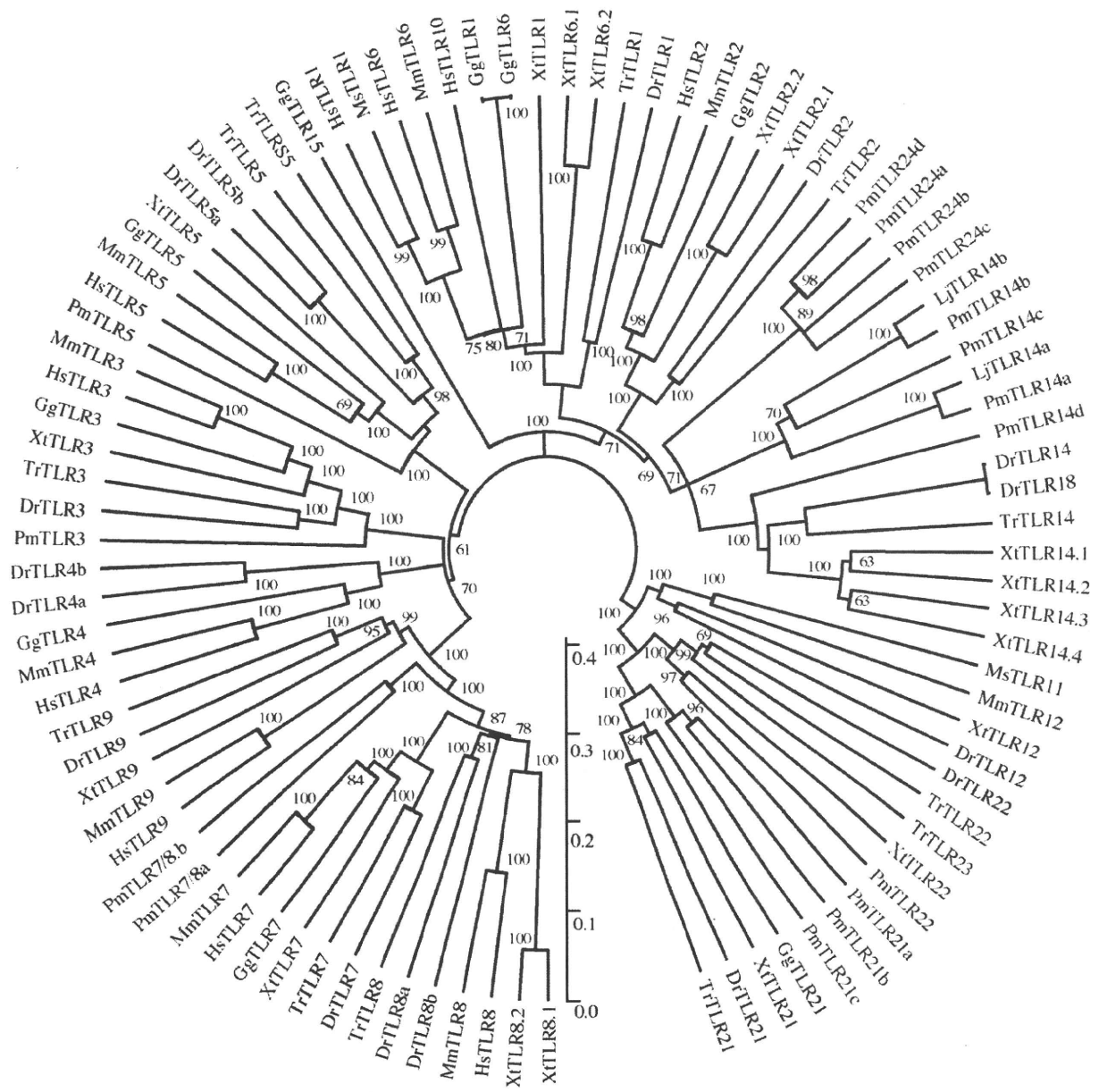

Fig. 2. Unrooted phylogenetic tree of vertebrate TLRs. The relationships were calculated on the basis of amino acid sequences of cytoplasmic TIR and extracellular LRR-regions. Bootstrap values (>60) are indicated. Hs; human (*Homo sapiens*), Mm; mouse (*Mus musculus*), Gg; chicken (*Gallus gallus*), Xt; frog (*Xenopus tropicalis*), Dr; zebrafish (*Danio rerio*), Tr; fugu (*T. rubripes*), Pm; Sea lamprey (*P. marinus*), Lj; Japanese lamprey (*L. japonicum*).

1b is the ortholog of jawed vertebrate TICAM-1 while pmTICAM-1a is either an ancestral or lamprey-specific TICAM gene.

3.4. Expression analysis of lamprey TLRs

RNA expressions of pmTLRs in several lamprey tissues were analyzed by RT-PCR. cDNA libraries were constructed from the eye, brain, gill, intestine, kidney, liver, muscle, skin, heart, and peripheral blood leukocytes (PBLs) from adult *L. japonicum* tissues. Each TLR primer set, except for pmTLR14a and b whose sequences were reported earlier (Ishii et al., 2007b), was derived from the nucleotide sequences of pmTLRs (Table 3). Almost all *L. japonicum* TLR cDNAs were successfully amplified using the sea lamprey primers, demonstrating that the sea lamprey and Japanese lamprey share similar TLR sets with very high homologies (Fig. 4). However, we could not amplify the TLR24c gene using any of the generated primer sets, nor could pmTLR24c be amplified using genomic DNA as a template. Further TBLASTN analysis using pmTLR24a as a query revealed that the N-terminal sequence of the TLR24c gene contained stop codon (data not shown), suggesting that ljTLR24c may in fact be a pseudogene, formed during the speciation of *P. marinus* and *L. japonicum* (Table 4).

The tissue distribution analysis indicated that every TLR mRNA was detected in each organ subjected to RT-PCR analyses (Fig. 4), although the level of expression differed among individual organs. All amplicons were sequenced and compared with sea lamprey TLR sequences by BLASTN analysis which revealed their partial nucleotide sequences were reasonably aligned with those predicted from the sea lamprey TLR genome (data not shown). Most lamprey TLR genes tended to be highly expressed in the gill, kid-

Please cite this article in press as: Kasamatsu, J., et al., Phylogenetic and expression analysis of lamprey toll-like receptors. Dev Comp Immunol (2010), doi:10.1016/j.dci.2010.03.004

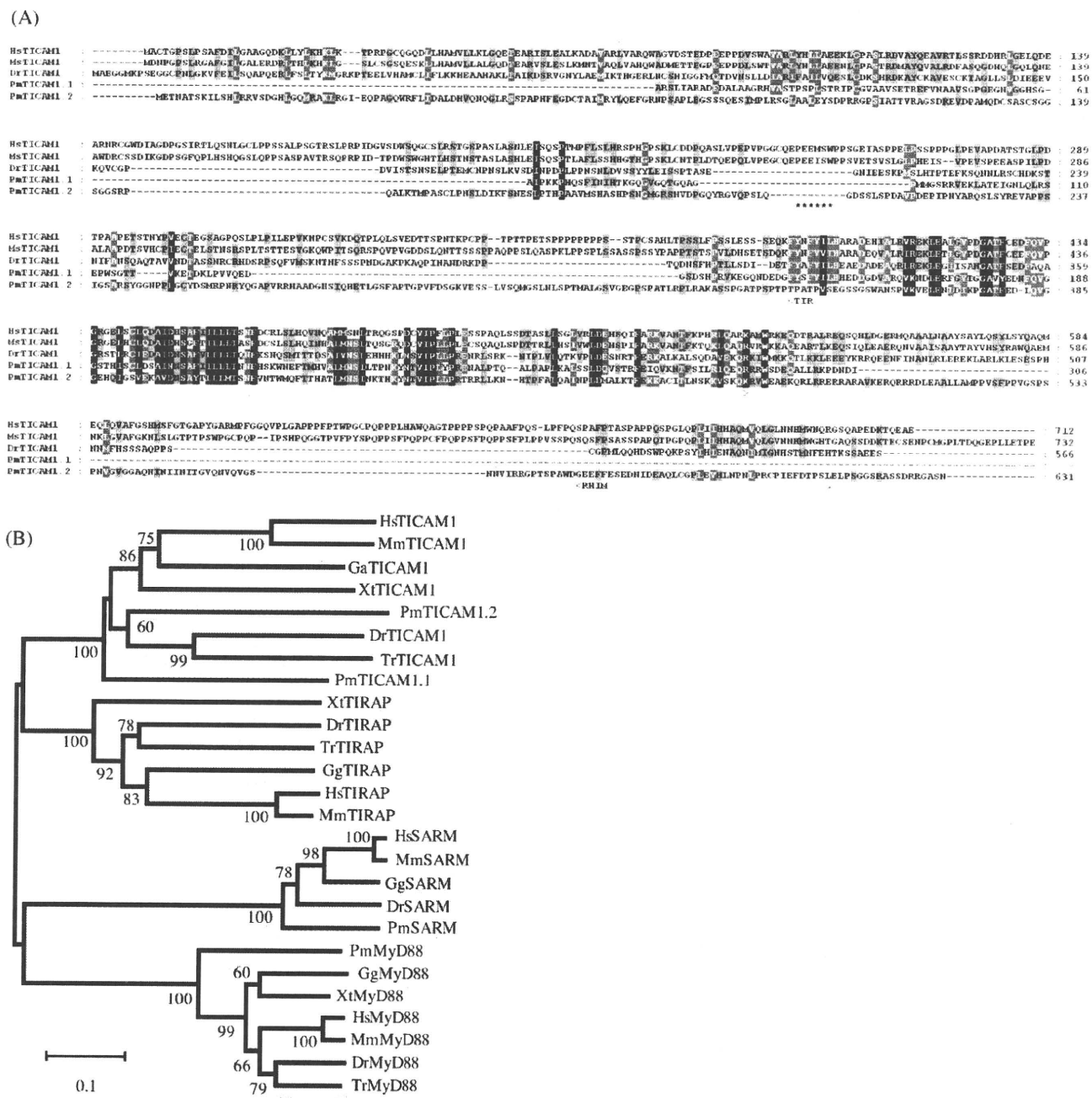

Fig. 3. (A) Alignment of vertebrate TICAM-1 sequences. An asterisk indicates the TRAF6-binding motif. Black shaded area, 100% identity; gray shaded area, 80–99% identity; light gray shaded area, 60–79% identity. (B) Unrooted phylogenetic tree of TIR-containing adaptors in vertebrates. The relationships were calculated on the basis of amino acid sequences of TIR domains. Bootstrap values (>60) are indicated. Hs; human (*H. sapiens*), Mm; mouse (*M. musculus*), Gg; chicken (*G. gallus*), Dr; zebrafish (*D. rerio*), Tr; fugu (*T. rubripes*), Pm; lamprey (*P. marinus*).

ney, and PBLs. Since these organs were rich in phagocytes and lymphocyte-like cells, TLRs may be dominantly expressed in the myeloid cells. Similarly, pmTICAM-1 adaptors were also expressed in the gill, kidney, and PBLs. Interestingly, pmTICAM-1a was predominantly expressed in the gill and PBLs, whereas pmTICAM-1b with the RHIM domain, was predominant in the kidney.

The ljTLR mRNA levels in PBLs were up- or down-regulated in response to polyI:C and heat-killed *E. coli*, which contain PAMPs (Fig. 5). ljTLR24a appeared to be transiently down-regulated while other ljTLRs were up-regulated 6 h after polyI:C stimulation. In contrast, *E. coli* stimulation tended to down-regulate mRNA levels of ljTLR3, 7/8b, 14b, and 21a. Thus, not only ljTLR3 but also ljTLR7/8a/b, 21a, 24b/c may be polyI:C-inducible genes and gene expression of most ljTLRs are controlled by exogenous microbial stimuli in lamprey.

4. Discussion

In this study, we annotated TLRs in the *P. marinus* genome using the latest assembled version of the Ensemble Lamprey Genome Browser database (released on August 2008), and determined their expression profiles by RT-PCR analyses within various organs in

Please cite this article in press as: Kasamatsu, J., et al., Phylogenetic and expression analysis of lamprey toll-like receptors. Dev Comp Immunol (2010), doi:10.1016/j.dci.2010.03.004

Table 3
Primers used in this study. The primers sets, excluding TLR14a and TLR14b, were constructed based on nucleotide sequences obtained from *P. marinus*.

Gene name	Forward primers (5′–3′)	Reverse primers (5′–3′)	PCR conditions (cycle and annealing temperature)
TLR2a	TGACTACCAATGCTCAAATCCAGAG	CCAGCTCAGGCAGGAGTTTC	35 cycles, 50 °C
TLR2b	CAACACACTACTGGGGATGAAACTAA	GTACCACAGCGCATCCAGGT	40 cycles, 50 °C
TLR2d	TCAATGCTCCAATCCAGAGAA	ATGATGTGGTGGCTGGGAAC	40 cycles, 50 °C
TLR14a	TCCTTGAGAGAGCTGTATCTGACG	AGTCCGAGTCCATGTGGCTGTAGG	40 cycles, 60 °C
TLR14b	TACATTGCACCCGAGTTGTACTCC	GTGGGCACCAGGGTGTTCTCCACC	45 cycles, 60 °C
TLR14c	TGGTCCCGACACTTGAGCAT	CGAGCGAGTCTTGGTTCTCC	40 cycles, 50 °C
TLR14d	CTACCGCTTCCACGCCTTC	GCTCGATGCTGTCGATGATG	35 cycles, 50 °C
TLR3	CGCTGTTCGTCCACTTTCA	GCTCCAGGTGTCTGCTCGTC	35 cycles, 50 °C
TLR5	CAGCATTGACCTCAGCCACA	GGCTATTGTTTGGGCTCCAC	40 cycles, 55 °C
TLR7/8a	TGCTACAATGCCCCTTACCC	GCCCTCAGCCAGTGCTTTT	35 cycles, 50 °C
TLR7/8b	GCTTCGACTGGTAGGGAATGG	CATCCCAAGGAATACGTGTCAG	35 cycles, 50 °C
TLR21a	GCGGTGTGCCAATCTTTCTC	TGGTTTCCACCCAGATCCAA	35 cycles, 50 °C
TLR21b	CCACGAGTTCCATGTGTCGT	CTTGAGGGTGATGAGGTTGCT	40 cycles, 50 °C
TLR21c	CCCCCAGTTGGAGAAAGAGG	ATGCGGTAGTAGGGCGACAG	35 cycles, 50 °C
TLR22	GTCTGCACCACCGCGACT	GCAGGTAGCTCCGCGTCA	35 cycles, 50 °C
MyD88	CACGTCCCGTAACAACAGCA	TGTCGGCGTAGCAGTAGCAG	33 cycles, 50 °C
TICAM1.1	GAGGGGCAGAATGATGAAGA	TTGTTCGGGGTTAGGATGGA	40 cycles, 50 °C
TICAM1.2	CTGGGCAGTACAGGGGTGTC	CGTCTCGTGCTGAATGCTGT	40 cycles, 50 °C
SARM	GCGATGAAGGAGAGCGTCA	CGCAGCAGTCCGTAGGTGT	35 cycles, 50 °C
EF1 alpha	CCATCGACATCTCTCTGTGGA	TAGTGCCGACGATGAGCTGCT	30 cycles, 60 °C

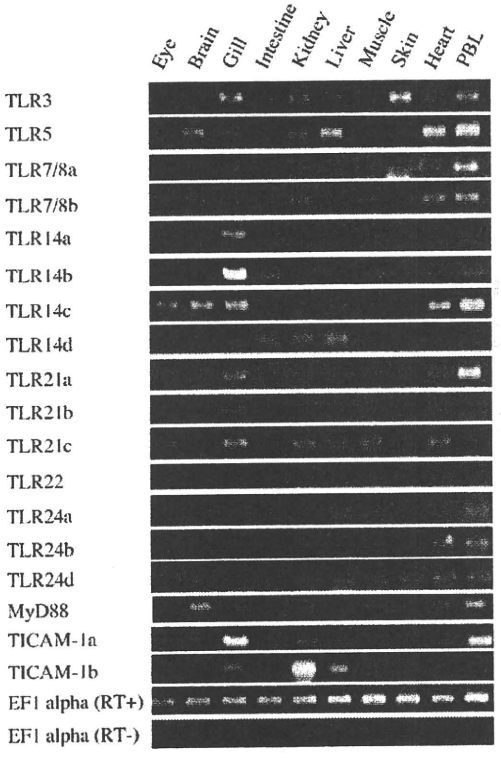

Fig. 4. Tissue expression profiles of *L. japonicum* TLR genes. All amplifications of the TLR cDNAs were performed by an identical PCR procedure. EF1 alpha was used as a positive control. No DNA was amplified by PCR regarding the EF1 alpha template from the non-reverse transcribed sample. Typical results were obtained using 30–45 PCR cycles.

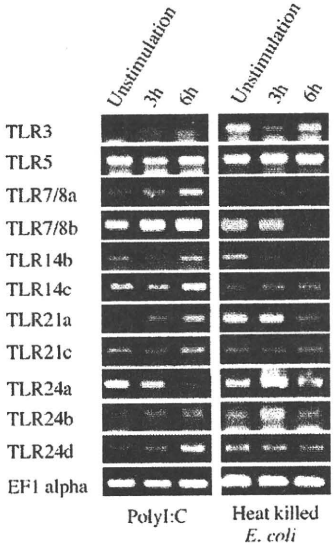

Fig. 5. Expression of blood cell ljTLRs in response to PAMP stimulation. Peripheral blood leukocytes were harvested from individuals of *L. japonicum*. Cells were separated into three groups: first group with no stimulation (unstimulation), second group with 3 h stimulation (3 h) and third group with 6 h stimulation. PolyI:C (10 μg/ml) and heat killed *E. coli* (3×10^7 cell/ml) were used as stimulators as indicated. EF1 was used as a positive control.

adult lampreys of *L. japonicum*. The overall features of the lamprey TLR system appear to resemble those of teleosts living in water in that they commonly express incomplete M-type TLRs and have more sophisticated F-type TLRs than land animals. The levels of ljTLRs in lamprey PBLs are regulated by PAMP stimuli as observed in mouse macrophages.

The prominent characteristics of the lamprey TLR system as compared to the teleost TLR system, are outlined below. We found three types of TLRs from the TLR2 subfamily in the lamprey, which correspond to TLR24 (pmTLR2a-d), TLR14 (pmTLR14a-c), and the ortholog of jawed vertebrate TLR14 (TLR14d), forming clearly distinct clusters in the phylogenetic tree. The TLR2 subfamily consists of multiple members displaying wide variability across animal species (Leulier and Lemaitre, 2008). Our past studies have shown that members of the chicken and amphibian TLR2 subfamily arose by lineage-specific duplication events (Ishii et al., 2007a; Higuchi et al., 2008). In combination with TLR2, human and mouse TLR1 and TLR6 facilitate the discrimination between triacylated and diacylated bacterial lipoproteins, respectively (Takeda et al., 2003). In contrast, chicken TLR2 proteins (chTLR1-1,2 and chTLR2-1,2) recognize bacterial lipoproteins and peptidoglycan in a different manner than human and mice (Higuchi et al., 2008). These studies suggest that divergence of the TLR2 subfamily seems to have developed by

Please cite this article in press as: Kasamatsu, J., et al., Phylogenetic and expression analysis of lamprey toll-like receptors. Dev Comp Immunol (2010), doi:10.1016/j.dci.2010.03.004

Table 4
Amino acid identities between human, mouse, zebrafish, and lamprey TICAM genes. Hs; human (*H. sapiens*), Mm; mouse (*M. musculus*), Dr; zebrafish (*D. rerio*), Pm; lamprey (*P. marinus*).

	HsTICAM-1	MmTICAM-1	DrTICAM-1	HsTICAM-2	MmTICAM-2	PmTICAM-1b
PmTICAM-1a	15.6%	14.0%	18.8%	18.2%	15.5%	18.9%
PmTICAM-1b	19.8%	19.3%	18.5%	9.4%	9.1%	–

gene duplication events and have allowed animals to specifically cope with pathogens sharing living environment with them.

Similarly, we also identified two TLR7/8 and three TLR21 genes in the lamprey genome. TLR3, 7, and 8, and teleost TLR22 recognize foreign RNA, while TLR9 and chicken TLR21 recognize unmethylated CpG DNAs (Matsuo et al., 2008; Brownlie et al., 2009). Therefore, our analysis indicates that lamprey has developed not only the TLR2 subfamily, but also other TLR proteins which recognize nucleic acids. This then begs the question: what was the original vertebrate TLR system? Table 5 shows a summary of the TLR repertoire present in deuterostomes. The TLR2 subfamily, TLR3, TLR5, TLR7/8, and TLR21/22 are essentially conserved in the lamprey and teleosts, suggesting that lampreys and jawed vertebrates conform to the same TLR family with hybrid M- and F-type TLRs, which may represent the origin of the TLR repertoire in vertebrates.

The vertebrate TLR phylogenetic tree in Fig. 2 appears as a star-like tree (Roach et al., 2005), and such a phylogram shape suggests that each TLR family was generated at the same time, which we termed the "TLR big-bomb". While the sea urchin and amphioxus possess approximately 200 (Hibino et al., 2006; Rast et al., 2006) and 50 TLRs (Holland et al., 2008; Huang et al., 2008), respectively, *C. intestinalis* has only 2 functional TLRs (Sasaki et al., 2009) identified from their genomes. In phylogenetic analyses of these studies, invertebrate TLRs did not clearly belong to vertebrate M- and F-type TLRs (Hibino et al., 2006; Holland et al., 2008; Huang et al., 2008; Sasaki et al., 2009). Therefore, M- and F-type TLRs may have arisen together with the origin of vertebrates. Interestingly, despite having only two TLRs, *C. intestinalis* can recognize a broad spectrum of PAMPs (Sasaki et al., 2009), indicating these unique invertebrate TLRs may have been an alternative origin of mammalian TLRs. In other words, vertebrate TLR proteins did not always recognize just one specific PAMP, but were able to recognize several PAMPs using a single type of M-type TLR (Sasaki et al., 2009). The gain or loss of these TLRs may have occurred during the evolution of vertebrates, although it is also possible that differential environmental factors promoted TLR divergence for animals to survive against microbial milieu, which although interesting to speculate, is beyond the scope of this analysis.

Our database analyses failed to identify orthologs of TLR4, 9 and 15, nor the TLR4-related genes, CD14, MD-2, and TIRAP in the Pre-Ensemble Lamprey Genome Browser database (Table 2). Absence of orthologs of CD14, MD-2 and TIRAP in lamprey may reflect the lack of a TLR4 system in lamprey as well as in teleosts and amphibia (Ishii et al., 2007a). It has long been established that teleosts are resistant to toxic effect of LPS. Recent study shows that zebrafish TLR4 acts as a negative regulator for NF-κB-signaling pathway, not for recognition of LPS (Sepulcre et al., 2009). Hence, these observations indicate that first the TLR4 gene arose in jawed vertebrates as a negative regulator of NF-κB-signaling pathway, and then it may have gained the function of LPS recognition with CD14 and MD-2 in an ancestor of amniota.

Additionally, we identified two TICAM genes, named TICAM-1a and b, in the lamprey genome. A previous study indicated that mammalian TICAM-1 and 2 genes resulted from two rounds of genome duplication, termed the 2R hypothesis, in early vertebrate evolution (Sullivan et al., 2007). In this hypothesis, one of the ancestral TICAM genes was lost after the first round of genome duplication, while after the second genome duplication, the TICAM-1 and 2 genes appeared. Although the timing of the genome duplications is still unclear (Kasahara, 2007; Panopoulou and Poustka, 2005), preliminary analyses of *HOX* gene clusters indicates the first round of genome duplication occurred in a common ancestor of jawed and jawless vertebrates (Irvine et al., 2002). In our analysis, pmTICAM-1b was identified as the

Table 5
TLR repertoires in deuterostomes.

	Human	Mouse	Chicken	Frog	Zebrafish	Fugu	Lamprey	Ascidian	Amphixus	Sea urchin
TLR1	+	+	+	+	+	+	–			
TLR2	+	+	+	+	+	+	+			
TLR3	+	+	+	+	+	+	+			
TLR4	+	+	+	+	+	–	–			
TLR5	+	+	+	+	+	+	+			
TLR6	+	+	*psd*	–	–	–	–			
TLR7	+	+	+	+	+	+	+			
TLR8	+	+	+	+	+	+	+	~27	~36?	~300?
TLR9	+	+	–	+	+	+	–			
TLR10	+	*psd*	–	–	–	–	–			
TLR12 (TLR11)	–	+	–	+	–	+	–			
TLR13	–	+	–	+	–	–	–			
TLR14 (TLR15)	–	–	+	+	+	+	+			
TLR21	–	–	–	+	+	+	+			
TLR22 (TLR23)	–	–	–	+	+	+	+			
TLR24	–	–	–	–	–	–	+			
MyD88	+	+	+	+	+	+	+	+	+	+
TICAM	+	+	+	+	+	+	+	–	+	–
RIG-I	+	+	+	+	+	+	+	+	+	–
MDA5	+	+	+	+	+	+	–	–	–	+
IPS-1	+	+	+	+	+	+	+	–	–	+
IRF3	+	+	–	+	+	+	–	–	–	–
IRF7	+	+	+	+	+	+	–	–	–	–
IFN	+	+	+	+	+	+	–	–	–	–

+; exists, –; does not exist, *psd*; pseudogene.

Please cite this article in press as: Kasamatsu, J., et al., Phylogenetic and expression analysis of lamprey toll-like receptors. Dev Comp Immunol (2010), doi:10.1016/j.dci.2010.03.004

ortholog of jawed vertebrate TICAM-1, whereas pmTICAM-1a did not show clear similarity to either TICAM-1 or TICAM-2. It is possible that pmTICAM-1a represents an ancestral gene of TICAM-2 that occurred during the first genome duplication event without gene loss. There are many TLRs binding to TICAM-1 in teleosts (Matsuo et al., 2008; Baoprasertkul et al., 2006), and TICAM-1a and b might have diverged due to the necessity for differential signaling of TICAM-associated TLRs in the lamprey.

Although the orthologs of nucleic acid-recognizing TLRs were predicted in the genome and confirmed by RT-PCR, no genes related to type I IFN induction except for the antiviral Mx gene were identified in the lamprey. While RIG-I/IPS-1, TBK1/IKKε and IRF-2, 4, 5, and 8 are present, genes corresponding to IRF-1, IRF-3, IRF-7, and type I IFN are not conserved in the lamprey genome (Table 2). The presence of the IFN-inducing pathway in lamprey is controversial as whole genome sequencing projects in ectoderms and primitive chordates, including sea urchin, amphioxus, and ascidian, have revealed the lack of type I IFN and its essential transcription factors, IRF-3 and IRF-7 (Table 5) (Hibino et al., 2006; Holland et al., 2008; Huang et al., 2008; Sasaki et al., 2009). Therefore, IFN-inducing pathway would be completed in a common ancestor of jawed vertebrates. Type I IFN plays a critical role in facilitating TCR-MHC-mediated lymphocyte activation of the acquired immune response in mammals. Although lamprey has many orthologs of jawed vertebrate TLRs and TLR-associated signaling molecules, it does not have MHC or authentic TCR/BCR.

Recent findings have indicated that lamprey possesses a unique acquired immune system involving variable lymphocyte receptors (VLRs) and the lymphoid system (Pancer and Cooper, 2006; Pancer et al., 2004; Flajnik, 2007; Kasahara et al., 2008). In agnathans, which includes lamprey and hagfish, clonally diversed receptors are generated by the assembly of genes for VLRA and VLRB, which are comprised of leucine-rich repeat (LRR) subunits and an invariant membrane-proximal stalk region (Pancer and Cooper, 2006; Pancer et al., 2005). Interestingly, the variable VLRA and VLRB products consist of a number of LRR motifs representing soluble forms and membrane-bound forms, respectively (Guo et al., 2009). Hence, the VLR-expressing lymphocytes are similar to authentic B and T cells in jawed vertebrates. Our study indicates that VLR-based acquired immunity may be regulated by TLRs with IFN-independent systems in jawless vertebrates. Functional analyses of lamprey TLRs need to be conducted in the future.

We can speculate from the current results that both water and land vertebrates possess common TLR proteins that may participate in the recognition of common PAMPs (Hirono et al., 2004). Indeed, lamprey also expresses a set of TLRs as in fish despite their evolutionary separation approximately 500 million years ago. The present results allow us to surmise that the TLR orthologs in lamprey and mammals recognize common PAMPs for host defense. The TLR system may serve to protect lampreys from infections despite the fact that their acquired immune system is modally different.

Acknowledgements

We are grateful to our laboratory members for invaluable discussions. This work was supported in part by Grants-in-Aid from the Ministry of Education, Science, and Culture (Specified Project for Advanced Research) of Japan and in part by the Program of Founding Research Centers for Emerging and Reemerging Infectious Diseases, MEXT. The supports by the Mitsubishi Foundation (TS), Takeda Foundation (TS) and Uehara memorial Foundation (MM) were gratefully acknowledged.

References

Baoprasertkul, P., Peatman, E., Somridhivej, B., Liu, Z., 2006. Toll-like receptor 3 and TICAM genes in catfish: species-specific expression profiles following infection with *Edwardsiella ictaluri*. Immunogenetics 58, 817–830.
Boyd, A., Philbin, V., Smith, A., 2007. Conserved and distinct aspects of the avian toll-like receptor (TLR) system: implications for transmission and control of bird-borne zoonoses. Biochem. Soc. Trans. 35, 1504–1507.
Brownlie, R., Zhu, J., Allan, B., Mutwiri, G., Babiuk, L., Potter, A., et al., 2009. Chicken TLR21 acts as a functional homologue to mammalian TLR9 in the recognition of CpG oligodeoxynucleotides. Mol. Immunol. 46, 3163–3170.
Flajnik, M., 2007. Immunogenetics: alternative strategies in adaptive immunity and the rise of comparative immunogenomics. Curr. Opin. Immunol. 19, 522–525.
Flajnik, M., Kasahara, M., 2001. Comparative genomics of the MHC: glimpses into the evolution of the adaptive immune system. Immunity 15, 351–362.
Guo, P., Hirano, M., Herrin, B., Li, J., Yu, C., Sadlonova, A., et al., 2009. Dual nature of the adaptive immune system in lampreys. Nature 459, 796–801.
Hibino, T., Loza-Coll, M., Messier, C., Majeske, A., Cohen, A., Terwilliger, D., et al., 2006. The immune gene repertoire encoded in the purple sea urchin genome. Dev. Biol. 300, 349–365.
Higuchi, M., Matsuo, A., Shingai, M., Shida, K., Ishii, A., Funami, K., et al., 2008. Combinational recognition of bacterial lipoproteins and peptidoglycan by chicken toll-like receptor 2 subfamily. Dev. Comp. Immunol. 32, 147–155.
Hirono, I., Takami, M., Miyata, M., Miyazaki, T., Han, H., Takano, T., et al., 2004. Characterization of gene structure and expression of two toll-like receptors from Japanese flounder, *Paralichthys olivaceus*. Immunogenetics 56, 38–46.
Holland, L., Albalat, R., Azumi, K., Benito-Gutiérrez, E., Blow, M., Bronner-Fraser, M., et al., 2008. The amphioxus genome illuminates vertebrate origins and cephalochordate biology. Genome Res. 18, 1100–1111.
Huang, S., Yuan, S., Guo, L., Yu, Y., Li, J., Wu, T., et al., 2008. Genomic analysis of the immune gene repertoire of amphioxus reveals extraordinary innate complexity and diversity. Genome Res. 18, 1112–1126.
Irvine, S., Carr, J., Bailey, W., Kawasaki, K., Shimizu, N., Amemiya, C., et al., 2002. Genomic analysis of Hox clusters in the sea lamprey *Petromyzon marinus*. J. Exp. Zool. 294, 47–62.
Ishii, A., Kawasaki, M., Matsumoto, M., Tochinai, S., Seya, T., 2007a. Phylogenetic and expression analysis of amphibian Xenopus toll-like receptors. Immunogenetics 59, 281–293.
Ishii, A., Matsuo, A., Sawa, H., Tsujita, T., Shida, K., Matsumoto, M., et al., 2007b. Lamprey TLRs with properties distinct from those of the variable lymphocyte receptors. J. Immunol. 178, 397–406.
Kasahara, M., 2007. The 2R hypothesis: an update. Curr. Opin. Immunol. 19, 547–552.
Kasahara, M., Kasamatsu, J., Sutoh, Y., 2008. Two types of antigen receptor systems in vertebrates. Zoolog. Sci. 25, 969–975.
Larkin, M., Blackshields, G., Brown, N., Chenna, R., McGettigan, P., McWilliam, H., et al., 2007. Clustal W and Clustal X version 2.0. Bioinformatics 23, 2947–2948.
Lemaitre, B., Nicolas, E., Michaut, L., Reichhart, J., Hoffmann, J., 1996. The dorsoventral regulatory gene cassette spätzle/Toll/cactus controls the potent antifungal response in Drosophila adults. Cell 86, 973–983.
Leulier, F., Lemaitre, B., 2008. Toll-like receptors – taking an evolutionary approach. Nat. Rev. Genet. 9, 165–178.
Liew, F., Xu, D., Brint, E., O'Neill, L., 2005. Negative regulation of toll-like receptor-mediated immune responses. Nat. Rev. Immunol. 5, 446–458.
Litman, G., Anderson, M., Rast, J., 1999. Evolution of antigen binding receptors. Annu. Rev. Immunol. 17, 109–147.
Matsuo, A., Oshiumi, H., Tsujita, T., Mitani, H., Kasai, H., Yoshimizu, M., et al., 2008. Teleost TLR22 recognizes RNA duplex to induce IFN and protect cells from birnaviruses. J. Immunol. 181, 3474–3485.
Medzhitov, R., Preston-Hurlburt, P., Janeway, C.J., 1997. A human homologue of the Drosophila toll protein signals activation of adaptive immunity. Nature 388, 394–397.
Oshiumi, H., Tsujita, T., Shida, K., Matsumoto, M., Ikeo, K., Seya, T., 2003a. Prediction of the prototype of the human toll-like receptor gene family from the pufferfish Fugu rubripes, genome. Immunogenetics 54, 791–800.
Oshiumi, H., Sasai, M., Shida, K., Fujita, T., Matsumoto, M., Seya, T., 2003b. TIR-containing adapter molecule (TICAM)-2, a bridging adapter recruiting to toll-like receptor 4 TICAM-1 that induces interferon-beta. J. Biol. Chem. 278, 49751–49762.
Oshiumi, H., Matsuo, A., Matsumoto, M., Seya, T., 2008. Pan-vertebrate toll-like receptors during evolution. Curr. Genomics 9, 488–493.
Pancer, Z., Cooper, M., 2006. The evolution of adaptive immunity. Annu. Rev. Immunol. 24, 497–518.
Pancer, Z., Amemiya, C., Ehrhardt, G., Ceitlin, J., Gartland, G., Cooper, M., 2004. Somatic diversification of variable lymphocyte receptors in the agnathan sea lamprey. Nature 430, 174–180.
Pancer, Z., Saha, N., Kasamatsu, J., Suzuki, T., Amemiya, C., Kasahara, M., et al., 2005. Variable lymphocyte receptors in hagfish. Proc. Natl. Acad. Sci. U.S.A. 102, 9224–9229.
Panopoulou, G., Poustka, A., 2005. Timing and mechanism of ancient vertebrate genome duplications – the adventure of a hypothesis. Trends Genet. 21, 559–567.
Rast, J., Smith, L., Loza-Coll, M., Hibino, T., Litman, G., 2006. Genomic insights into the immune system of the sea urchin. Science 314, 952–956.
Roach, J., Glusman, G., Rowen, L., Kaur, A., Purcell, M., Smith, K., et al., 2005. The evolution of vertebrate toll-like receptors. Proc. Natl. Acad. Sci. U.S.A. 102, 9577–9582.

Please cite this article in press as: Kasamatsu, J., et al., Phylogenetic and expression analysis of lamprey toll-like receptors. Dev Comp Immunol (2010), doi:10.1016/j.dci.2010.03.004

Sasaki, N., Ogasawara, M., Sekiguchi, T., Kusumoto, S., Satake, H., 2009. Toll-like receptors of the ascidian *Ciona intestinalis*: prototypes with hybrid functionalities of vertebrate toll-like receptors. J. Biol. Chem. 284, 27336–27343.

Sepulcre, M., Alcaraz-Pérez, F., López-Muñoz, A., Roca, F., Meseguer, J., Cayuela, M., et al., 2009. Evolution of lipopolysaccharide (LPS) recognition and signaling: fish TLR4 does not recognize LPS and negatively regulates NF-kappaB activation. J. Immunol. 182, 1836–1845.

Seya, T., Matsumoto, M., 2009. The extrinsic RNA-sensing pathway for adjuvant immunotherapy of cancer. Cancer Immunol. Immunother. 58, 1175–1184.

Seya, T., Matsumoto, M., Ebihara, T., Oshiumi, H., 2009. Functional evolution of the TICAM-1 pathway for extrinsic RNA sensing. Immunol. Rev. 227, 44–53.

Sullivan, C., Postlethwait, J., Lage, C., Millard, P., Kim, C., 2007. Evidence for evolving toll-IL-1 receptor-containing adaptor molecule function in vertebrates. J. Immunol. 178, 4517–4527.

Takeda, K., Kaisho, T., Akira, S., 2003. Toll-like receptors. Annu. Rev. Immunol. 21, 335–376.

Tamura, K., Dudley, J., Nei, M., Kumar, S., 2007. MEGA4: molecular evolutionary genetics analysis (MEGA) software version 4.0. Mol. Biol. Evol. 24, 1596–1599.

Please cite this article in press as: Kasamatsu, J., et al., Phylogenetic and expression analysis of lamprey toll-like receptors. Dev Comp Immunol (2010), doi:10.1016/j.dci.2010.03.004

Cancer Science
The official journal of the Japanese Cancer Association JCA

Adjuvant engineering for cancer immunotherapy: Development of a synthetic TLR2 ligand with increased cell adhesion

Takashi Akazawa,[1,2,5] Norimitsu Inoue,[1] Hiroaki Shime,[1,3] Ken Kodama,[4] Misako Matsumoto[2,3] and Tsukasa Seya[2,3]

Departments of [1]Molecular Genetics, [2]Immunology, Osaka Medical Center for Cancer and Cardiovascular Diseases, Osaka; [3]Department of Microbiology and Immunology, Hokkaido University Graduate School of Medicine, Sapporo; [4]Department of Surgery, Osaka Medical Center for Cancer and Cardiovascular Diseases, Osaka, Japan

(Recieved August 21, 2009/Revised December 8, 2009; March 23, 2010/Accepted March 28, 2010/Accepted manuscript online April 5, 2010/Article first published online May 7, 2010)

The development of effective immunoadjuvants for tumor immunotherapy is of fundamental importance. The use of *Mycobacterium bovis* bacillus Calmette-Guérin cell wall skeleton (BCG-CWS) in tumor immunotherapy has been examined in various clinical applications. Because BCG-CWS is a macromolecule that cannot be chemically synthesized, the development of an alternative synthetic molecule is necessary to ensure a constant supply of adjuvant. In the present study, a new adjuvant was designed based on the structure of macrophage-activating lipopeptide (MALP)-2, which is a Toll-like receptor (TLR)-2 ligand similar to BCG-CWS. Macrophage-activating lipopeptide-2, [S-(2,3-bispalmitoyloxypropyl)Cys (P2C) – GNNDESNISFKEK], originally identified in a Mycoplasma species, is a lipopeptide that can be chemically synthesized. A MALP-2 peptide was substituted with a functional motif, RGDS, creating a novel molecule named P2C-RGDS. RGDS was selected because its sequence constitutes an integrin-binding motif and various integrins are expressed in immune cells including dendritic cells (DCs). Thus, this motif adds functionality to the ligand. P2C-RGDS activated DCs and splenocytes more efficiently than MALP-2 over short incubation times *in vitro*, and the RGDS motif contributed to their activation. Furthermore, P2C-RGDS showed higher activity than MALP-2 in inducing migration of DCs to draining lymph node, and in inhibiting tumor growth *in vivo*. This process of designing and developing synthetic adjuvants has been named "adjuvant engineering," and the evaluation and improvement of P2C-RGDS constitutes a first step in the development of stronger synthetic adjuvants in the future. (*Cancer Sci* 2010; 101: 1596–1603)

Bacterial adjuvants that were used as biological response modifiers (BRM) for cancer immunotherapy in the 1970s have recently been re-evaluated.[1–3] Cancer antigens that had been identified in many laboratories were tested as peptide vaccines for clinical applications, but the peptides alone were not sufficient to fully activate the immune system.[4] These results suggested that the activation of the innate immune system, including dendritic cells (DCs), by a supporting adjuvant was important.[5–8] In peptide vaccine therapy, the T cells of the acquired immune system play an important role in recognizing and attacking tumor cells.[9] Dendritic cells play a key role in the regulation of the acquired immune system by presenting antigen and inducing a primary immune response. The identification of the Toll-like receptor (TLR) family advanced the understanding of DC function and of the role of adjuvants, because almost all microbial adjuvants work as TLR ligands and activate DCs.[10–12] These findings provide the basis for the understanding of the mechanism of adjuvant therapy.

Dr Azuma developed BCG-CWS, a cell-wall skeleton preparation of *Mycobacterium bovis* bacillus Calmette-Guérin,[13,14] as an antitumor immunotherapeutic adjuvant. Although many BRM studies have been discontinued, basic and clinical research on BCG-CWS has continued at Osaka Medical Center for Cancer. We reported that BCG-CWS is a ligand of TLR2/4[15–17] and acts as an effective adjuvant to induce CTLs in irradiated tumors in a mouse experimental model. These activities are mediated by the myeloid differentiation protein 88 (MyD88),[18] which is a TLR adaptor molecule. The effectiveness of BCG-CWS in improving the prognosis for cancer patients after surgery was confirmed through clinical research.[19]

Interleukin (IL)-23 and interferon (IFN)-γ are the main cytokines induced by BCG-CWS *in vivo*[14,19,20] and are important for antitumor immunity.[21,22] Interleukin-12 is well known as an antitumor cytokine,[23] and IL-23 shares the IL12p40 subunit with IL-12.[22] Unexpectedly, IL-23 advanced tumor growth in experiments with IL-23R$^{-/-}$ mice or neutralizing antibodies by interacting with Th17 cells.[24–26] However, systemic administration of IL-23 was also reported to have antitumor effects similar to those of IL-12,[27] and TLR2 ligands exhibit antitumor activity[28–30] that may be mediated by the induction of IL-23.

Although BCG-CWS is effective as an adjuvant, its clinical use is limited in purity, stability, and a stable supply because it cannot be chemically synthesized and is therefore prepared from bacterial cells. These factors indicate that there is a need to develop new synthetic adjuvants as effective as BCG-CWS. The present report describes the design of such adjuvants based on the structure of the TLR2 ligand and in consideration of the need for IL-23 induction. Macrophage-activating lipopeptide (MALP)-2, a lipopeptide of mycoplasmic origin, is a TLR2 ligand that can be chemically synthesized. No functional consensus peptide sequences were identified in MALP-2. The N-terminal cysteine of the 13-amino-acid peptide of bacterial origin was modified with 2 palmitates [Pam2Cys or P2C, S-(2,3-bispalmitoyloxypropyl)-cysteine],[31] but P2C alone does not work as a TLR2 ligand.[32] Bacterial and synthetic TLR2 ligands (MALP-2, FSL-1,[32] P2C-SKKKK[33]) contain mostly hydrophilic peptides, and the presence of solubilizers critically affects their TLR2 agonistic ability,[34] suggesting that the activity of compounds as TLR2 agonists correlates with their solubility.

CD11c is a member of the integrin superfamily and is known to be a marker of DCs.[35] Dendritic cells also express other integrin molecules such as αV/β3 and α5/β1, and the RGDS motif specifically binds to these integrins.[36,37] Virus particles expressing proteins containing the RGD motif efficiently infect DCs.[37] Therefore, a new TLR2 ligand was developed by

[5]To whom correspondence should be addressed.
E-mail: akazawa-ta@mc.pref.osaka.jp

doi: 10.1111/j.1349-7006.2010.01583.x

replacing the peptide of bacterial origin with a hydrophilic functional motif (adjuvant engineering). P2C and the RGDS peptide were linked to increase the efficiency of ligand adherence to DCs or other immune cells, and the effect of the new adjuvant on antitumor activities *in vitro* and *in vivo* was examined.

Materials and Methods

Mice, cells, and reagents. Toll/IL-1 receptor homology-containing adaptor molecule (TICAM)-$1^{-/-}$ mice were generated in our laboratory.[2] Toll-like receptor (TLR)-$2^{-/-}$ and MyD88$^{-/-}$ mice were provided by Shizuo Akira (Osaka University).[38] The mice were maintained under specific pathogen-free conditions in the animal facility of the Osaka Medical Center. They were backcrossed with C57BL/6 mice >8 times before use. Wild-type (WT) C57BL/6 mice were purchased from Japan Clea (Tokyo, Japan). All animal experiments were approved by the committee at Osaka Medical Center for Cancer. EG7 cells are ovalbumin-transfected EL4 and were obtained from the American Type Culture Collection (ATCC, Manassas, VA, USA).[39] B16D8 was established in our laboratory as a subline of the B16 melanoma cell line.[18] Cell lysates were prepared by the freeze-thaw method.

Preparation of mouse bone marrow-derived DCs (BMDCs), splenocytes, and lymph node cells. Bone marrow-derived DCs were prepared as previously described[35,40] with minor modifications, and were cultured in RPMI-1640 (Invitrogen, Carlsbad, CA, USA) containing 10 ng/mL mouse granulocyte-macrophage colony-stimulating factor (PeproTech EC, London, UK), 50 μM 2-mercaptoethanol (Invitrogen), 10 mM HEPES, and 10% FCS (Bio Whittaker, Walkersville, MD, USA). The inguinal lymph node cells and splenocytes were prepared by using Lympholyte-M (Cedarlane, Burlington, ON, Canada). CD11c-positive and -negative cells, and CD90-positive and -negative cells were separated from splenocytes by using CD11c or CD90 microbeads (Miltenyi Biotec, Auburn, CA, USA).

***In vitro* assay.** For the simple stimulation assay *in vitro*, BMDCs or splenocytes were cultured with 10 μg/mL of BCG-CWS,[18] 100 nM of MALP-2 and the designed lipopeptide (purity >90%; Biologica, Aichi, Japan) for 24 h (BMDCs, FACS), 48 h (BMDCs, ELISA), or 72 h (splenocytes, ELISA). For the inhibition assay, BMDCs or splenocytes were pre-incubated with the indicated concentrations of RGDS peptide or anti-CD29 antibody (eBioscience, San Diego, CA, USA) at 4°C for 30 min before stimulating them with TLR2 ligands at 4°C for 60 min. The cells were then washed and re-cultured for 48 h (BMDCs, ELISA) or 72 h (splenocytes, ELISA). The Mixed Lymphocyte Reaction (MLR) assay was performed as previously described,[40] and the results were analyzed as uptake of [^{3}H]thymidine (1 μCi/well; Amersham Biosciences, Piscataway, NJ, USA). Bone marrow-derived DCs stimulated with TLR2 ligands for 24 h (C57BL/6, 5×10^4 cells) were co-cultured with CD90-positive T cells (BALB/c, 10^5 cells) for 72 h. To exclude the possible effect of contaminating lipopolysaccharide, lipopeptides were pretreated with polymyxin B (Sigma-Aldrich, St. Louis, MO, USA) at 37°C for 60 min.

Fluorescence-activated cell sorter (FACS) analysis, intracellular cytokine staining, and ELISA. For FACS analysis, cells were suspended in PBS containing 0.1% sodium azide and 1% FCS, and then incubated for 30 min at 4°C with FITC-conjugated anti-mouse CD80, antimouse CD86, antimouse CD8, or isotype control antibody; or with phycoerythrin-conjugated antimouse CD4 or isotype control antibody (eBioscience). The cells were washed, and their fluorescence intensities were measured by FACS analysis. For intracellular cytokine staining, splenocytes were stimulated with P2C-RGDS for 72 h and Brefeldin A (GolgiPlug; BD Biosciences, San Diego, CA, USA) for the last 6 h. Cells were stained with phycoerythrin-conjugated antimouse CD3e, antimouse CD4, antimouse CD8a antibodies, allophycocyanin-conjugated antimouse CD11c, or antimouse NK1.1 antibodies (eBioscience), followed by fixation and permeabilization with the Cytofix/Cytoperm plus Kit (BD Biosciences). Cells were stained intracellularly with FITC-labeled anti-IFN-γ antibody (XMG1.2; eBioscience). For ELISA, samples were stored at –80°C and analyzed with ELISA kits for IFN-γ, TNF-α, and IL12p40 (Biosource, Camarillo, CA, USA).

***In vivo* therapy model.** C57BL/6 mice were shaved on the back and injected subcutaneously with 200 μL of $1–2 \times 10^6$ syngeneic EG7 cells in PBS on Day 0. Thereafter, the treatment was performed three times, on Days 16, 20, and 23, and tumor volumes were measured using a caliper every 2–3 days. A volume of 50 μL of a mixture consisting of 10 nmol of lipopeptide and the cell lysate of 2×10^5 EG7 cells with or without 10 nmol of RGDS peptide was injected intradermally around the transplanted tumor. Tumor volume was calculated using the formula: Tumor volume (cm^3) = (long diameter) × (short diameter) × (short diameter) × 0.4. Statistical analysis was performed with the Student's *t*-test.

***Ex vivo* assay.** C57BL/6 mice were treated intradermally with a mixture of 10 nmol of lipopeptide and the cell lysate of 2×10^5 EG7 cells every 3 days for >4 treatments. At 24 h after the last treatment, the mice were sacrificed by etherization, and then the splenocytes and lymph node cells were prepared and cultured for 4 days to be primed by DCs and macrophages. The cytolytic activities of lymph node cells were then analyzed with a ^{51}Cr release assay.[18] The percentage of specific lysis was calculated using the formula: %Specific lysis = [(experimental release – spontaneous release)/(total release – spontaneous release)] × 100. The proportions of CD8- and CD11c-positive cells in the lymph nodes or spleen were analyzed by FACS.

Results

To design a new TLR2 ligand with activity equivalent to that of BCG-CWS, the minimum lipopeptide unit, P2C, was connected to the RGDS integrin-binding motif to increase adherence to DCs, forming P2C-RGDS (Fig. 1a). The hydrophobicity and pI of P2C-RGDS were similar to those of MALP-2, and the molecular weight of P2C-RGDS was half that of MALP-2 (Fig. 1b).

First, the synthetic adjuvants were tested for their capacity to activate BMDCs *in vitro* when these compounds were added to the culture medium. P2C-RGDS enhanced the expression of CD80 and CD86 in BMDCs at a level equal to that of MALP-2, the positive control (Fig. 2a). P2C-RGDS also enhanced the production of IL12p40 and TNF-α (Fig. 2b) and the proliferation of allogeneic T cells co-cultured with the BMDCs. Thus, P2C-RGDS and MALP-2 stimulate DCs equally *in vitro*, whereas P2C does not show the same activity.

Macrophage-activating lipopeptide-2 is a ligand of TLR2/6 that activates DCs through MyD88. To examine the TLR2 and TLR signaling pathway-dependence of P2C-RGDS, BMDCs were prepared from TLR2$^{-/-}$, MyD88$^{-/-}$, or TICAM-$1^{-/-}$ mice and stimulated with these synthetic lipopeptides. Both MALP-2 and P2C-RGDS enhanced the expression of CD80 and CD86 in BMDCs derived from WT or TICAM-$1^{-/-}$ mice, but not TLR2$^{-/-}$ or MyD88$^{-/-}$ mice (Fig. 3), suggesting that P2C-RGDS is a TLR2 ligand with activity similar to that of MALP-2 *in vitro*.

Next, the functional dependence of P2C-RGDS as a TLR2 ligand on not only its hydrophilicity, but also on the motif-specificity of the peptide sequences, was tested. Since MALP2 and P2C-RGDS activated DCs to the same extent at 37°C for 48 h, DCs were instead stimulated at 4°C for 1 h, then washed and re-cultured at 37°C for 48 h. Under these conditions, P2C-RGDS induced IL12p40 more efficiently than MALP-2 (Fig. 4a). To analyze the specificity of the RGDS peptide,

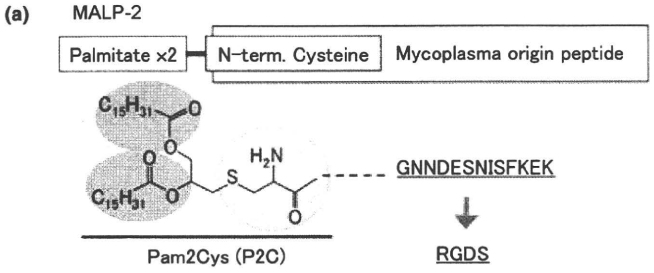

(b)

Compounds		M.W.	Peptide	pI	Hydrophobicity
P2C		672.5	P2 C	—	—
MALP-2	(N)	2134.1	P2 C G N N D E S N I S F K E K	*4.68	−1.5
FSL-1	(N)	1666.1	P2 C G D P K H P K S F	8.21	−1.36
P2C-SKKKK	(S)	1271.8	P2 C S K K K K	10.04	−2.32
P2C-RGDS	(S)	1087.5	P2 C R G D S	*5.83	−1.34

Fig. 1. The structure of the adjuvant developed in the present study, a synthetic Toll-like receptor (TLR)-2 ligand containing the RGDS motif. (a) The structure of macrophage-activating lipopeptide (MALP)-2. The N-terminal cysteine of a peptide derived from a mycobacterium is modified with 2 palmitates [Pam2Cys, P2C, S-(2,3-bispalmitoyloxypropyl)cysteine]. RGDS was conjugated to P2C to form P2C-RGDS because of its hydrophilicity and its additional function as an integrin-binding motif for cell adhesion. (b) The structure, molecular weight, isoelectric point (pI), and hydrophobicity of synthetic (P2C-RGDS, P2C-SKKKK) and natural (MALP-2, FSL-1) lipopeptides used in this study. The pI and hydrophobicity of the peptide were calculated using ProtParam tools (http://br.expasy.org/tools/protparam.html). The pI and hydrophobicity of P2C-RGDS were almost equivalent to those of MALP-2. The molecular weight of P2C-RGDS was about half that of MALP-2. N, natural TLR2 ligand; S, synthetic TLR2 ligand. The asterisks (*) indicate acidic peptides. The gray boxes indicate hydrophobic amino acids.

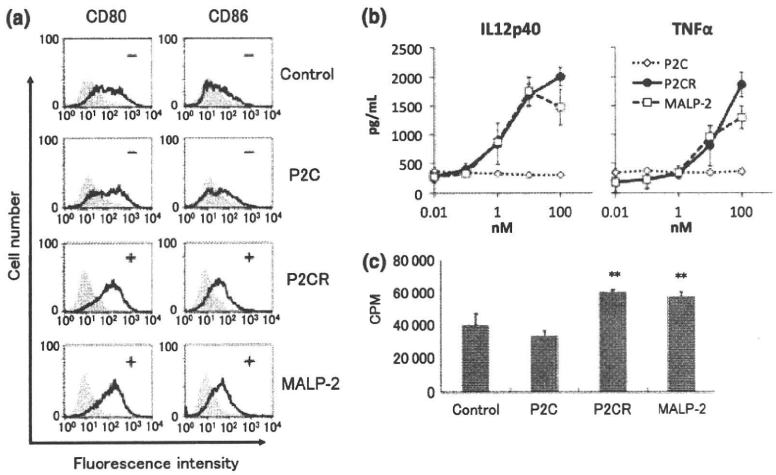

Fig. 2. P2C-RGDS activates bone marrow-derived dendritic cells (BMDCs) as much as macrophage-activating lipopeptide (MALP)-2 *in vitro*. (a) The enhancement of CD80/CD86 expression of BMDCs stimulated with the indicated compounds (100 nM) for 24 h was observed by FACS analysis. (b) Interleukin (IL)12p40 and tumor necrosis factor (TNF)-α production in BMDCs stimulated with each compound for 48 h was determined by ELISA. (c) The proliferation of allogeneic T cells co-cultured with activated-BMDCs for 72 h was measured by the [^{3}H] thymidine uptake method. Bone marrow-derived dendritic cells were treated with each compound for 24 h before co-culture with T cells. CPM, count per minute. $^{**}P < 0.01$ *vs* control (Student's *t*-test). P2CR, P2C-RGDS.

IL12p40 production was inhibited by the addition of an RGDS competitor peptide or anti-integrin β1 antibody to the assay. The addition of the RGDS competitor peptide and the integrin blocking antibodies partially attenuated the production of IL12p40 induced by P2C-RGDS, but not that induced by MALP-2 (Fig. 4b,c). These results indicate that not only hydrophilicity but also the functional RGDS motif contributes to the activation of DCs *in vitro* at short incubation times.

The P2C-RGDS-induced production of IFN-γ was evaluated next, using *in vitro* whole splenocyte stimulation. The activities of P2C-RGDS and MALP-2, as measured by IFN-γ production, were comparable and weaker than that of BCG-CWS when splenocytes were simply stimulated with each compound for 72 h (Fig. 5a). However, when splenocytes were stimulated with each compound at 4°C for 1 h and re-cultured at 37°C for 72 h, the P2C-RGDS-induced production of IFN-γ was stronger than that induced by MALP-2 and it was attenuated mostly by the RGDS peptide. Furthermore, the splenocytes stimulated with P2C-RGDS produced as much IFN-γ as those stimulated with BCG-CWS at 4°C for 1 h (Fig. 5b). Interferon-γ production was not detected in splenocytes depleted of CD11c-positive dendritic cells, and IFN-γ production could be restored under these conditions by adding back CD11c-positive cells. These data indicate that IFN-γ production by splenocytes following stimulation with

doi: 10.1111/j.1349-7006.2010.01583.x

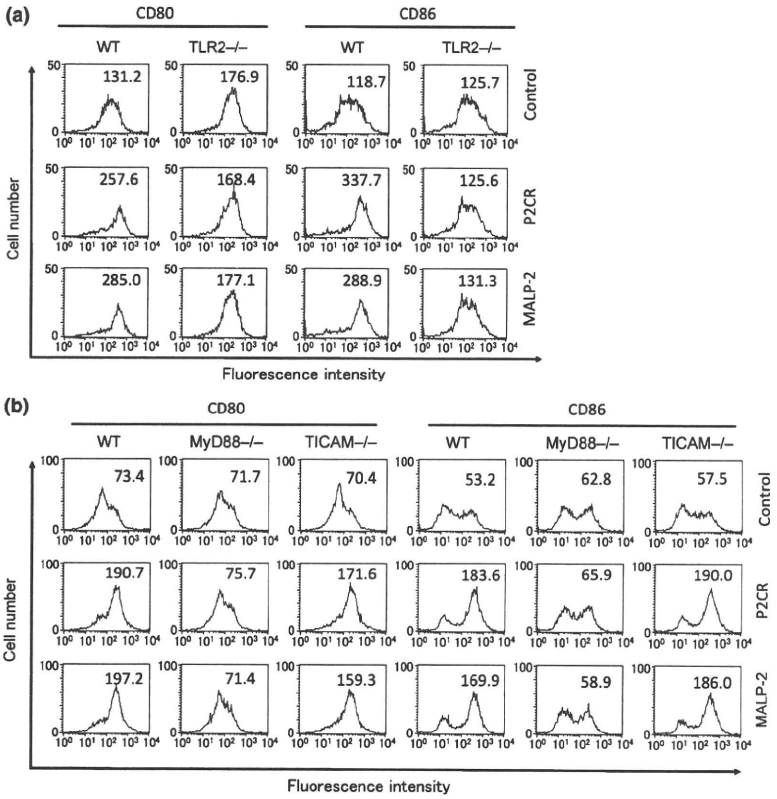

Fig. 3. P2C-RGDS activates bone marrow-derived dendritic cells (BMDCs) in a Toll-like receptor (TLR)-2 and myeloid differentiation protein (MyD)-88-dependent manner *in vitro*. (a,b) Bone marrow-derived dendritic cells were prepared from mice lacking TLR2 ($TLR2^{-/-}$) and TLR adaptor molecules ($MyD88^{-/-}$ and TICAM-$1^{-/-}$). CD80 and CD86 expression was observed by FACS analysis at 24 h after BMDCs were stimulated with MALP-2 or P2C-RGDS. The numbers in the panels represent mean fluorescence intensities. P2C-RGDS and MALP-2 activated BMDCs via TLR2 and MyD88, but not via the Toll/IL-1 receptor homology-containing adaptor molecule (TICAM)-1 pathway. P2CR, P2C-RGDS.

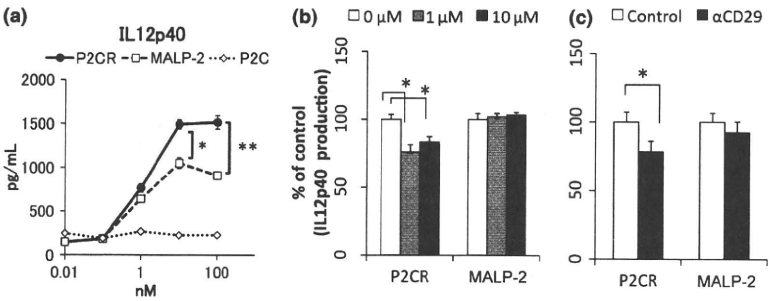

Fig. 4. P2C-RGDS efficiently activates bone marrow-derived dendritic cells (BMDCs) in an RGDS motif–dependent manner *in vitro* over short incubation times. (a) Interleukin (IL)12p40 production of BMDCs stimulated with each Toll-like receptor (TLR)-2 ligand at 4°C for 1 h. Bone marrow-derived dendritic cells were washed after the stimulation and re-cultured for 48 h. Interleukin12p40 production was determined by ELISA. (b) Bone marrow-derived dendritic cells were pretreated with the indicated concentrations of RGDS peptide (P2C-modification free) as a competitor at 4°C for 30 min. Then, the BMDCs were stimulated with TLR2 ligands (10 nM) at 4°C for 1 h. Interleukin12p40 production by BMDCs was determined by ELISA. Data are shown as percentages of each control value. (c) The inhibition effects of α-CD29 (integrin β1) antibody on IL12p40 production of BMDCs. Bone marrow-derived dendritic cells were pre-treated with 10 μg/mL of each antibody at 4°C for 30 min before stimulation. P2CR, P2C-RGDS.

P2C-RGDS was mediated by DC activation (Fig. 5c). IFN-γ production was also impaired by depletion of CD90 (Thy1)-positive T cells (Fig. 5c). Further assessment of IFN-γ producing cells by intracellular cytokine staining revealed that IFN-γ was mainly detected in CD3- or CD8-positive cells, and in CD4-, NK1.1-, or CD11c-negative cells stimulated with P2C-RGDS (Fig. 5d).

Finally, the antitumor activity of P2C-RGDS *in vivo* was investigated using a tumor-implantation model. The mice were transplanted with EG7 on day 0, and treated with synthetic lipopeptide (10 nmol) and the cell lysate of EG7 cells (2×10^5) on Days 16, 20, and 23. The minimum lipopeptide unit P2C showed no *in vivo* antitumor activity similar to the activation of DCs *in vitro*. Although MALP-2-treated mice showed a slightly smaller tumor volume than control mice, this difference was not significant. However, P2C-RGDS showed a significant antitumor effect (Student's *t*-test, $P < 0.05$ *vs* control; Fig. 6a). Moreover, the mixture of P2C and the RGDS peptide showed no antitumor activity (Fig. 6b). Next, lymph node cells from mice immunized with EG7 lysate and P2C-RGDS or MALP-2 were isolated, and the cytotoxicity against EG7 and B16D8 cells was measured using a ^{51}Cr release assay. P2C-RGDS specifically

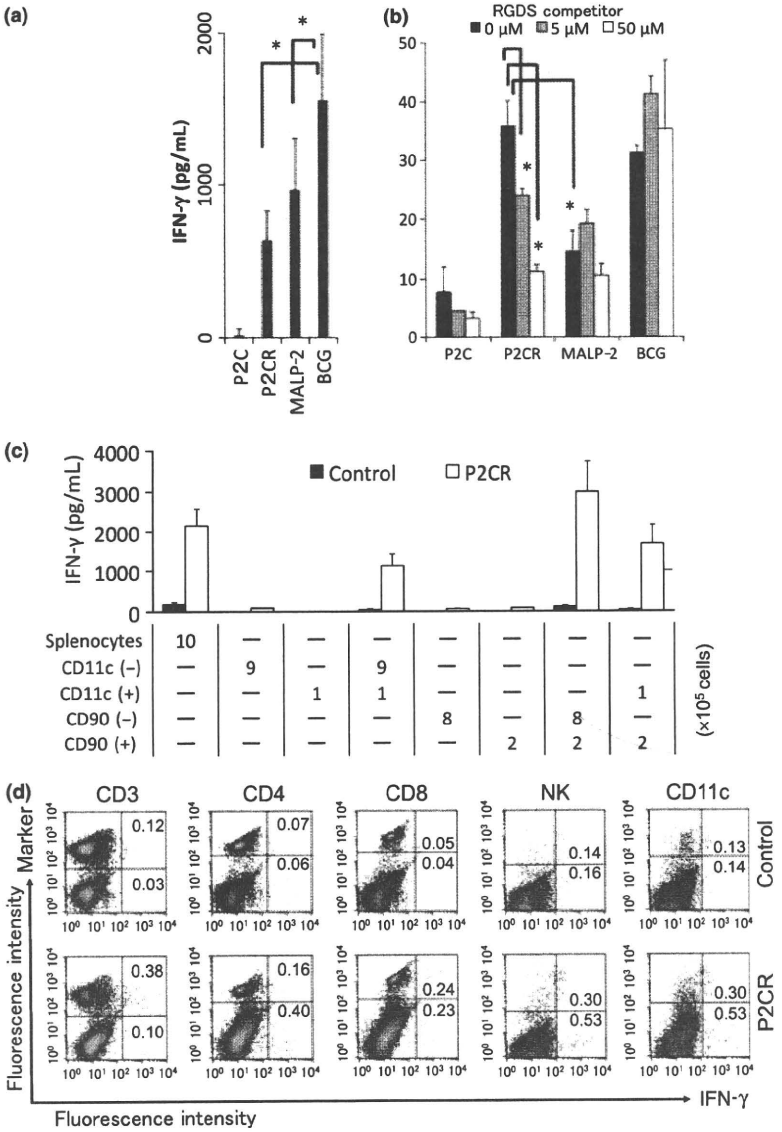

Fig. 5. P2C-RGDS efficiently activates splenocytes in an RGDS motif-dependent manner. (a) Interferon (IFN)-γ production by splenocytes stimulated with each compound for 72 h. (b) The effect of RGDS competitor peptide pretreatment on IFN-γ production. The RGDS competitor attenuated IFN-γ production from splenocytes stimulated with P2C-RGDS at 4°C for 1 h. (c) The roles of CD11c-positive cells (dendritic cells) and CD90-positive cells (T cells) on IFN-γ production by splenocytes. The splenocytes were separated into $CD11c^+$ and $CD11c^-$ cells, or $CD90^+$ and $CD90^-$ cells by using MACS beads. Cells were prepared based on the recovery ratio and stimulated with P2C-RGDS for 72 h. $^*P < 0.05$, $^{**}P < 0.01$ (Student's *t*-test); n.d, not detected. (d) Intracellular IFN-γ staining of splenocytes with various expression markers. Density plots show the expression of each surface marker and intracellular staining for IFN-γ, and the numbers indicate the proportion of IFN-γ-positive cells (%). P2CR, P2C-RGDS.

induced a stronger cytotoxic activity against EG7 than MALP-2, but the lymph node cells were not sufficiently cytotoxic against the negative target B16D8 cells (Fig. 6c). In addition, lymph node cells were cultured continuously with live EG7 cells for 96 h and the proportion of CD8-positive cells was analyzed by FACS. CD8-positive cells in lymph nodes derived from P2C-RGDS-treated mice remained at a level of approximately 16% of total cells, but most CD8-positive cells from MALP-2-treated mice were lost after culture with EG7 (Fig. 6d). The proportion of CD8-positive cells in a splenocyte population derived from immunized mice was also evaluated using FACS analysis. CD8-positive cells were proportionally higher among splenocytes derived from mice treated with P2C-RGDS than among splenocytes derived from mice treated with MALP-2 (Fig. 6e). Necrosis was observed on the surface of tumors after P2C-RGDS but not after MALP-2 treatment, and CD8-positive cells were detected around the necrosis tissue by immunostaining (data not shown). These data suggest that P2C-RGDS induces and activates CTLs more efficiently than MALP-2. Moreover, to analyze the mechanism underlying the strong antitumor effect of P2C-RGDS *in vivo*, the proportions of CD11c-positive cells in draining lymph nodes were analyzed in mice treated with MALP-2 or P2C-RGDS for 24 h. P2C-RGDS induced the migration of CD11c-positive cells to the draining lymph nodes more effectively than MALP2 ($P = 0.055$, Fig. 6f).

Discussion

Natural TLR2 ligands of bacterial origin, such as MALP-2[31,41,42] and FSL-1,[32] have been reported to effectively activate CD8-positive T cells and induce antitumor activity. Because these lipopeptides are hydrophilic, it was predicted that the hydrophilicity of the peptide might be important for its activity.[31–34] Several researchers have relied on a chemobiologic strategy of producing amino acid replacements to explore which portion of the lipopeptide sequence possesses effective adjuvant activity.[43] Using this strategy, Takeda developed Tan-1511 analogues that show high levels of activity in the induction of granulopoiesis.[43] Another strategy has been to randomly search for sequences or peptides effective at enhancing TLR2 ligand

doi: 10.1111/j.1349-7006.2010.01583.x

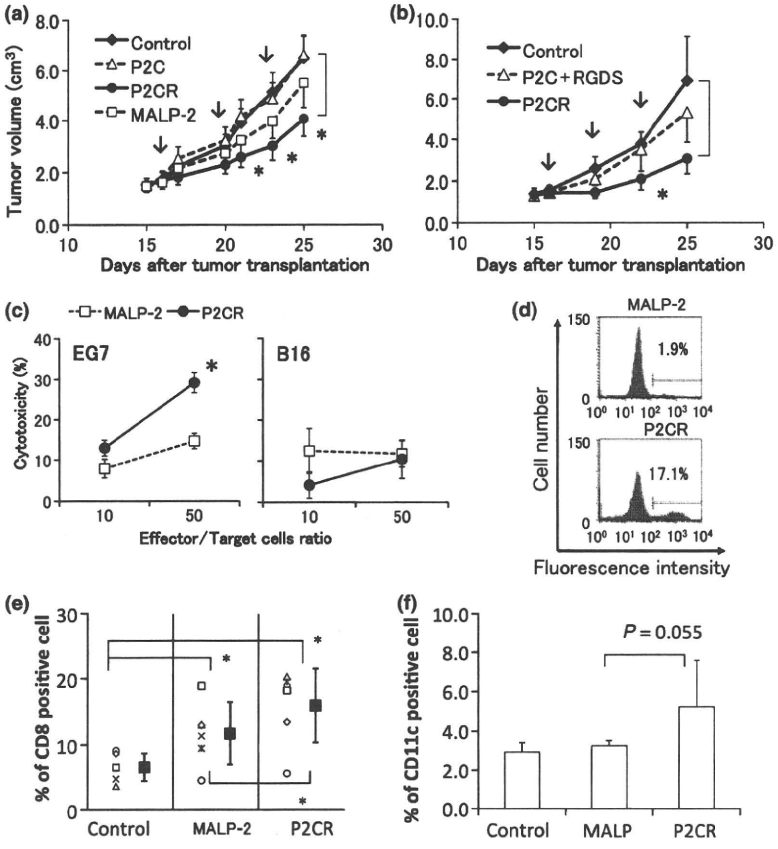

Fig. 6. P2C-RGDS is more effective at retarding tumor growth and inducing CD8-positive cells than macrophage-activating lipopeptide (MALP)-2 *in vivo* and *ex vivo*. Antitumor effect of P2C-RGDS and MALP-2 (a), and of a mixture of P2C and RGDS peptide (b), in the EG7-implanted mouse model (C57BL6-EG7 model). Mice were treated with Toll-like receptor (TLR)-2 ligand and EG7 lysate on Days 16, 20, and 23 (arrows). The data are shown as means ± SE ($n = 9$). $^*P < 0.05$ *vs* control (Student's *t*-test). (c) Lymph node cells derived from P2C-RGDS and EG7 lysate-immunized mice showed stronger cytotoxicity than cells from MALP-2-immunized mice against EG7 but not B16 (^{51}Cr release assay). $^*P < 0.05$ *vs* MALP-2 (Student's *t*-test). (d) CD8-positive T cells were more effectively induced in lymph nodes derived from mice immunized with P2C-RGDS and EG7 lysate than in those immunized with MALP-2. The lymph node cells in Figure 6(c) were cultured with live EG7 for 96 h, and then the proportion of CD8-positive T cells was analyzed. (e) Immunization with P2C-RGDS and EG7 lysate induced CD8-positive T cells in splenocytes more efficiently than immunization with MALP-2. The proportions of CD8-positive cells in splenocytes were determined by FACS analysis at 96 h after the initiation of splenocyte cultivation. Each symbol indicates an individual experiment. The closed squares represent average ± SD. $^*P < 0.05$ (paired *t*-test). (f) The proportion of CD11c-positive cells in the draining lymph nodes at 24 h after immunization. CD11c-positive cells were examined by FACS analysis. $P = 0.055$ *vs* MALP-2 (Student's *t*-test). P2CR, P2C-RGDS.

activity.[44] The purpose of the current project was to design a TLR2 ligand with an additional function through the addition of a hydrophilic, functional peptide that could be developed as a new synthetic adjuvant (Fig. 1). In comparison to a prior developmental strategies, the present design has the advantage of allowing the selection of various functions, and because the designed lipopeptides do not exist in nature, they could show new or enhanced properties. In the present study, the TLR2 ligand was designed to possess stronger adhesive capacity through the linking of the RGDS peptide to P2C.

The compound P2C-RGDS was developed and shown to be as effective as MALP-2 in generating BMDC responses *in vitro*, such as the enhancement of a maturation marker (CD80 and CD86) and cytokine induction when DCs were cultured with each compound for 24–48 h (Fig. 2). P2C-RGDS and MALP-2 also activated DCs through the TLR2–MyD88 pathway (Fig. 3),[38] but P2C-RGDS activated DCs more efficiently than MALP2, and the RGDS integrin binding motif was found to be important for DCs activation over short incubation times (Fig. 4). Because DCs were treated with compounds for only 1 h, then washed and re-cultured at 37°C for 48 h in these experiments, it was predicted that P2C-RGDS might efficiently adhere to the DCs in short incubation times, and then stimulate DCs continuously at the surface or in the phagosome of DCs. Whole splenocytes stimulated with P2C-RGDS also produced more IFN-γ than MALP-2 over short incubation times (Fig. 5b), and the production of IFN-γ by splenocytes depended on CD11c-positive DCs (Fig. 5c). These data suggest that the adhesion properties of P2C-RGDS caused the efficient activation of DCs, and reflected splenocyte activation. The stronger IFN-γ induction by P2C-RGDS might also be due to its retention in the culture system by adherence to various cells among the splenocytes. Moreover, P2C-RGDS may be retained in local regions for a long time via integrin binding *in vivo*, leading to the efficient activation of immune cells such as dermal DCs. P2C-RGDS induced the migration of CD11c-positive cells into the draining lymph nodes more effectively than MALP-2 in *in vivo* experiments (Fig. 6f). These DCs might activate CD8-positive cells, enhance cytotoxicity (Fig. 6c), and lead to retardation of tumor growth (Fig. 6a). These data suggest that the greater activation of DCs by P2C-RGDS compared to MALP2 influences IFN-γ production by splenocytes, thereby resulting in increased cytotoxicity and antitumor effects *in vivo*.

The induction of IFN-γ production by BCG-CWS treatment is one of the indexes for continuing treatment in clinical applications,[14,19] and the response can be confirmed in mouse experiments. Interferon-γ stimulation up-regulates the expression of MHC class I in tumor cells,[45] presumably improving tumor recognition by immune cells, and leading to increased suppression of tumor growth. With short stimulation periods, P2C-RGDS induced as much IFN-γ as BCG-CWS. Although the present compound was designed without considering IFN-γ induction, results show that CD8-positive cells produced IFN-γ in splenocytes stimulated with P2C-RGDS alone in the absence of antigen peptide (Fig. 5). The mechanism of IFN-γ induction by P2C-RGDS should be analyzed in the future. The tumor volume of the BCG-CWS treatment group was about 60% of that of the control on Day 22 (data not shown), and the therapeutic effects of P2C-RGDS were almost equivalent to those of BCG-CWS. Because BCG-CWS must be emulsified with drakeol, the use of P2C-RGDS has significant advantages.

The integrin binding sequence has served as the basis for the design of drugs that depend on adhesive activity. In the present work, this adhesive function was applied to TLR ligands to enhance immunoadjuvant activity. Cilengitide, a cyclic RGD peptide, was developed as an integrin αV antagonist, which impairs angiogenesis, tumor growth, and metastasis[46] because integrins are expressed on various tumor cells.[47] Although EG7 expresses integrin αV, β1, and β3, P2C-RGDS and RGDS peptide did not show direct cytotoxic activity against EG7 cells at concentrations up to 100 nM (data not shown). Furthermore, the adjuvant activities of P2C-RGDS were compared to those of a mixture of P2C and RGDS peptide. P2C had no adjuvant activity, such as the activation of DCs and splenocytes *in vitro* or antitumor effect *in vivo* by lipopeptides (Figs 2b, 5a, 6a). The mixture did not show any effects *in vivo* such as appreciable antitumor activity (Fig. 6b). Based on these results, the stronger antitumor activity of P2C-RGDS compared to that of MALP-2 is thought to occur through an increase in cell adhesive ability, but not through the inhibition of angiogenesis.

Concerning the relationship between TLR and its ligand, it is suggested that a co-receptor plays a key role for TLR binding and signaling[1,7,48] as observed previously for CD14 in the Lipopolysaccharide (LPS)–TLR4 signaling pathway. Although integrin binding is predicted to support the capture and phagocytosis of ligands by DCs, integrin signaling in addition to TLR signaling might influence adjuvant activity. Stronger adjuvants will be developed by selecting for other properties, in addition to TLR signaling, that are essential for adjuvant activity, and the integrin signal could be one of the candidates.

In the present work, the inclusion of an integrin-binding motif in a TLR2 ligand was examined for its effect in increasing the activity of the compound as an antitumor adjuvant by enhancing adhesion of the ligand to DCs and other cells. Dendritic cells efficiently recognized P2C-RGDS, which they adhered to and maintained around cells, and P2C-RGDS showed stronger antitumor activity than MALP-2 *in vivo*. The present adjuvant-engineering project is a new strategy to incorporate biological findings into drug design. Targeting peptides are used to elicit a strictly selective response among immune cells. A targeted strategy can effectively activate immune cells at a low concentration while not affecting other cells whose activation might lead to side effects. More than 20 TLR2 ligands with 10 alternative functions have already been synthesized by adjuvant engineering and our group is working to develop the strongest adjuvant through continued evaluation and improvements.

Acknowledgments

This work was supported in part by KAKENHI (15790069; 19790301; 20200075; 21790400) from the Ministry of Education, Culture, Science, and Technology of Japan; The Uehara Memorial Foundation; Osaka Community Foundation; and The Charitable Trust Osaka Cancer Researcher Fund. We are grateful to Drs K. Toyoshima, H. Koyama, S. Imaoka, S. Hori, K. Kato, and M. Tatsuta (Osaka Medical Center for Cancer, Osaka) for their support of this work. We are grateful to Dr K. Kikuchi (Sapporo Medical University, Sapporo), who gave the name "adjuvant engineering" to our project. Thanks are also due to N. Kanto, and T. Yasuda, E. Takahara, Y. Mimura, and M. Yabu (Osaka Medical Center for Cancer, Osaka) for their assistance.

References

1 Seya T, Akazawa T, Tsujita T, Matsumoto M. Role of Toll-like receptors in adjuvant-augmented immune therapies. *Evid Based Complement Alternat Med* 2006; **3**(1): 31–8.
2 Akazawa T, Ebihara T, Okuno M *et al.* Antitumor NK activation induced by the Toll-like receptor 3-TICAM-1 (TRIF) pathway in myeloid dendritic cells. *Proc Natl Acad Sci U S A* 2007; **104**(1): 252–7.
3 Okamoto M, Oshikawa T, Tano T *et al.* Involvement of Toll-like receptor 4 signaling in interferon-g production and antitumor effect by streptococcal agent OK-432. *J Natl Cancer Inst* 2003; **95**(4): 316–26.
4 Rosenberg SA, Yang JC, Restifo NP. Cancer immunotherapy: moving beyond current vaccines. *Nat Med* 2004; **10**(9): 909–15.
5 Celis E. Toll-like receptor ligands energize peptide vaccines through multiple paths. *Cancer Res* 2007; **67**(17): 7945–7.
6 Kanzler H, Barrat FJ, Hessel EM, Coffman RL. Therapeutic targeting of innate immunity with Toll-like receptor agonists and antagonists. *Nat Med* 2007; **13**(5): 552–9.
7 Seya T, Akazawa T, Uehori J, Matsumoto M, Azuma I, Toyoshima K. Role of toll-like receptors and their adaptors in adjuvant immunotherapy for cancer. *Anticancer Res* 2003; **23**(6a): 4369–76.
8 Akira S, Uematsu S, Takeuchi O. Pathogen recognition and innate immunity. *Cell* 2006; **124**: 783–801.
9 Miconnet I, Coste I, Beermann F *et al.* Cancer vaccine design: a novel bacterial adjuvant for peptide-specific CTL induction. *J Immunol* 2001; **166**(7): 4612–19.
10 Iwasaki A, Medzhitov R. Toll-like receptor control of the adaptive immune responses. *Nat Immunol* 2004; **5**: 987–95.
11 Kaisho T, Akira S. Toll-like receptors as adjuvant receptors. *Biochim Biophys Acta* 2002; **1589**(1): 1–13.
12 Hemmi H, Takeuchi O, Kawai T *et al.* A Toll-like receptor recognizes bacterial DNA. *Nature* 2000; **408**(6813): 740–5.
13 Azuma I, Ribi EE, Meyer TJ, Zbar B. Biologically active components from mycobacterial cell walls: I Isolation and composition of cell wall skeleton and component P3. *J Natl Cancer Inst* 1974; **52**: 95–101.
14 Hayashi A, Doi O, Azuma I, Toyoshima K. Immuno-friendly use of BCG-cell wall skeleton remarkably improves the survival rate of various cancer patients. *Proc Jpn Acad* 1998; **74** Ser. B: 50–5.
15 Uehori J, Fukase K, Akazawa T *et al.* Dendritic cell maturation induced by muramyl dipeptide (MDP) derivatives: monoacylated MDP confers TLR2/TLR4 activation. *J Immunol* 2005; **174**(11): 7096–103.
16 Tsuji S, Matsumoto M, Takeuchi O *et al.* Maturation of human dendritic cells by cell wall skeleton of Mycobacterium bovis bacillus Calmette-Guérin: involvement of toll-like receptors. *Infect Immun* 2000; **68**: 6883–90.
17 Uehori J, Matsumoto M, Tsuji S *et al.* Simultaneous blocking of human Toll-like receptor 2 and 4 suppresses myeloid dendritic cell activation induced by Mycobacterium bovis bacillus Calmette-Guérin (BCG)-peptidoglycan (PGN). *Infect Immun* 2003; **71**: 4238–49.
18 Akazawa T, Masuda H, Saeki Y *et al.* Adjuvant-mediated tumor regression and tumor-specific cytotoxic response are impaired in MyD88-deficient mice. *Cancer Res* 2004; **64**(2): 757–64.
19 Kodama K, Higashiyama M, Takami K *et al.* Innate immune therapy with a Bacillus Calmette-Guérin cell wall skeleton after radical surgery for non-small cell lung cancer: a case-control study. *Surg Today* 2009; **39**(3): 194–200.
20 Begum NA, Ishii K, Kurita-Taniguchi M *et al.* Mycobacterium bovis BCG cell wall-specific differentially expressed genes identified by differential display and cDNA subtraction in human macrophages. *Infect Immun* 2004; **72**(2): 937–48.
21 Matsumoto M, Seya T, Kikkawa S *et al.* Interferon gamma-producing ability in blood lymphocytes of patients with lung cancer through activation of the innate immune system by BCG cell wall skeleton. *Int Immunopharmacol* 2001; **1**(8): 1559–69.
22 Oppmann B, Lesley R, Blom B *et al.* Novel p19 protein engages IL-12p40 to form a cytokine, IL-23, with biological activities similar as well as distinct from IL-12. *Immunity* 2000; **13**(5): 715–25.
23 Zou JP, Yamamoto N, Fujii T *et al.* Systemic administration of rIL-12 induces complete tumor regression and protective immunity: response is correlated with a striking reversal of suppressed IFN-g production by anti-tumor T cells. *Int Immunol* 1995; **7**(7): 1135–45.
24 Langowski JL, Zhang X, Wu L *et al.* IL-23 promotes tumour incidence and growth. *Nature* 2006; **442**(7101): 461–5.
25 Kolls JK, Lindén A. Interleukin-17 family members and inflammation. *Immunity* 2004; **21**(4): 467–76.
26 Shime H, Yabu M, Akazawa T *et al.* Tumor-secreted lactic acid promotes IL-23/IL-17 proinflammatory pathway. *J Immunol* 2008; **180**(11): 7175–83.
27 Kaiga T, Sato M, Kaneda H, Iwakura Y, Takayama T, Tahara H. Systemic administration of IL-23 induces potent antitumor immunity primarily mediated through Th1-type response in association with the endogenously expressed IL-12. *J Immunol* 2007; **178**(12): 7571–80.
28 Jackson DC, Lau YF, Le T *et al.* A totally synthetic vaccine of generic structure that targets Toll-like receptor 2 on dendritic cells and promotes

doi: 10.1111/j.1349-7006.2010.01583.x

antibody or cytotoxic T cell responses. *Proc Natl Acad Sci U S A* 2004; **101**(43): 15440–5.
29 Schneider C, Schmidt T, Ziske C *et al.* Tumour suppression induced by the macrophage activating lipopeptide MALP-2 in an ultrasound guided pancreatic carcinoma mouse model. *Gut* 2004; **53**(3): 355–61.
30 Murata M. Activation of Toll-like receptor 2 by a novel preparation of cell wall skeleton from Mycobacterium bovis BCG Tokyo (SMP-105) sufficiently enhances immune responses against tumors. *Cancer Sci* 2008; **99**(7): 1435–40.
31 Mühlradt PF, Kiess M, Meyer H, Süssmuth R, Jung G. Isolation, structure elucidation, and synthesis of a macrophage stimulatory lipopeptide from Mycoplasma fermentans acting at picomolar concentration. *J Exp Med* 1997; **185**(11): 1951–8.
32 Okusawa T, Fujita M, Nakamura J *et al.* Relationship between structures and biological activities of mycoplasmal diacylated lipopeptides and their recognition by toll-like receptors 2 and 6. *Infect Immun* 2004; **72**(3): 1657–65.
33 Omueti KO, Beyer JM, Johnson CM, Lyle EA, Tapping RI. Domain exchange between human toll-like receptors 1 and 6 reveals a region required for lipopeptide discrimination. *J Biol Chem* 2005; **280**(44): 36616–25.
34 Voss S, Ulmer AJ, Jung G, Wiesmüller KH, Brock R. The activity of lipopeptide TLR2 agonists critically depends on the presence of solubilizers. *Eur J Immunol* 2007; **37**(12): 3489–98.
35 Inaba K, Pack M, Inaba M, Sakuta H, Isdell F, Steinman RM. High levels of a major histocompatibility complex II-self peptide complex on dendritic cells from the T cell areas of lymph nodes. *J Exp Med* 1997; **186**: 665–72.
36 Harui A, Roth MD, Vira D, Sanghvi M, Mizuguchi H, Basak SK. Adenoviral-encoded antigens are presented efficiently by a subset of dendritic cells expressing high levels of aV-b3 integrins. *J Leukoc Biol* 2006; **79**(6): 1271–8.
37 Okada N, Masunaga Y, Okada Y *et al.* Gene transduction efficiency and maturation status in mouse bone marrow-derived dendritic cells infected with conventional or RGD fiber-mutant adenovirus vectors. *Cancer Gene Ther* 2003; **10**(5): 421–31.
38 Kaisho T, Takeuchi O, Kawai T, Hoshino K, Akira S. Endotoxin-induced maturation of MyD88-deficient dendritic cells. *J Immunol* 2001; **166**(9): 5688–94.
39 Helmich BK, Dutton RW. The role of adoptively transferred CD8 T cells and host cells in the control of the growth of the EG7 thymoma: factors that determine the relative effectiveness and Homing properties of Tc1 and Tc2 effectors. *J Immunol* 2001; **166**: 6500–8.
40 Akazawa T, Shingai M, Sasai M *et al.* Tumor immunotherapy using bone marrow-derived dendritic cells overexpressing Toll-like receptor adaptors. *FEBS Lett* 2007; **581**(18): 3334–40.
41 Matsumoto M, Nishiguchi M, Kikkawa S, Nishimura H, Nagasawa S, Seya T. Structural and functional properties of complement-activating protein M161Ag, a Mycoplasma fermentans gene product that induces cytokine production by human monocytes. *J Biol Chem* 1998; **273**: 12407–14.
42 Nishiguchi M, Matsumoto M, Takao T *et al.* Mycoplasma fermentans lipoprotein M161Ag-induced cell activation is mediated by Toll-like receptor 2: role of N-terminal hydrophobic portion in its multiple functions. *J Immunol* 2001; **166**: 2610–16.
43 Hida T, Hayashi K, Yukishige K, Tanida S, Kawamura N, Harada S. Synthesis and biological activities of TAN-1511 Analogues. *J Antibiot* 1995; **48**(7): 589–603.
44 Reutter F, Jung G, Baier W, Treyer B, Bessler WG, Wiesmüller KH. Immunostimulants and Toll-like receptor ligands obtained by screening combinatorial lipopeptide collections. *J Pept Res* 2005; **65**(3): 375–83.
45 Gobin SJ, Peijnenburg A, Keijsers V, van den Elsen PJ. Site a is crucial for two routes of IFN g-induced MHC class I transactivation: the ISRE-mediated route and a novel pathway involving CIITA. *Immunity* 1997; **6**(5): 601–11.
46 Buerkle MA, Pahernik SA, Sutter A, Jonczyk A, Messmer K, Dellian M. Inhibition of the alpha-nu integrins with a cyclic RGD peptide impairs angiogenesis, growth and metastasis of solid tumours *in vivo*. *Br J Cancer* 2002; **86**(5): 788–95.
47 Janssen ML, Oyen WJ, Dijkgraaf I *et al.* Tumor targeting with radiolabeled alpha(v)beta(3) integrin binding peptides in a nude mouse model. *Cancer Res* 2002; **62**(21): 6146–51.
48 Seya T, Matsumoto M, Tsuji S, Begum NA, Azuma I, Toyoshima K. Structural-functional relationship of pathogen-associated molecular patterns: lessons from BCG cell wall skeleton and mycoplasma lipoprotein M161Ag. *Microbes Infect* 2002; **4**(9): 955–61.

Vaccine 28 (2010) 8041–8042

Contents lists available at ScienceDirect

Vaccine

journal homepage: www.elsevier.com/locate/vaccine

Innate immunity and vaccine

Tsukasa Seya*

Department of Microbiology and Immunology, Hokkaido University Graduate School of Medicine, Kita-ku, Kita 15, Nishi 7, Sapporo 060-8638, Japan

ARTICLE INFO

Article history:
Received 23 February 2010
Accepted 26 April 2010
Available online 17 September 2010

Keywords:
TLR
MyD88
TICAM-1 (TRIF)
Dendritic cells
NK activation

ABSTRACT

Immune adjuvant is an artificial pathogen-associated molecular patterns (PAMP) for potentiating various immune responses. Vaccine represents one event that is capable of inducing immune response caused by antigen and PAMP stimuli, which act on antigen-presenting dendritic cells (mDCs). Here, we introduce the pathways by which CTL and NK cells are driven through mDC maturation in response to adjuvants.

Microbial pattern molecules (PAMP, pathogen-associated molecular patterns) are agonists of pattern-recognition receptors, a representative of which is Toll-like receptor. Adjuvants belong to non-infectious artificial PAMP, typically administered with the target antigen (Ag) in order to enhance the host immune response [1]. However, the mechanism by which these reagents enhance immunity had not clearly been understood, until the recent progress on elucidation of the ligand properties of Toll-like receptors (TLRs) and TLR-mediated DC maturation [2]. The accumulating evidence on TLR-dependent DC maturation has solidified the current understanding that DC TLRs participate in determining what kind of effector cells are driven by the DCs that present antigens. Now, we hold that Ags determine the object toward which immune cells are proliferated whereas adjuvant determines what effectors will be selected for immunological output [1]. The fundamental concepts of the immune system should be re-evaluated through the understanding of TLR-mediated DC immune responses, which will also revolutionize the concepts related to vaccination.

In myeloid DCs (mDCs), a representative Ag-presenting cells, the two major arms of the innate immune signaling pathway, the MyD88 and TICAM-1 (Toll-IL-1 receptor homology domain-containing adaptor molecule, also named TRIF) pathways, have been identified through the investigation of TLR signaling [2]. TLR3 represents the sensor of dsRNA of viral origin and recruits TICAM-1 [3]. TICAM-1 links the type I IFN-inducing pathways in mDCs of both human and mouse [2,3]. TLR4 recruits both MyD88 and TICAM-1 [2]. TLRs other than TLR3 can take the MyD88 pathway. Hence, the representative inflammatory responses in TLR pattern-recognition are rooted in the properties of the adaptors MyD88 and TICAM-1. In myeloid DCs, these pathways play a significant role in differential maturation.

Using BCG-cell wall skeleton (CWS) as the TLR2/4 adjuvant, we found that MyD88 is an adaptor essential for induction of cross-priming in mDCs [4]. MyD88−/− mice have been reported to far less induction of CTL against exogenous Ags and TLR2/4 adjuvants [4]. Cytokines and NF-κB-inducing factors may be required for mDC cross-priming, although the molecular mechanism whereby MyD88 can induce responses related to cross-presentation in mDCs is undetermined.

We have used polyI:C for evaluating the TICAM-1 (TRIF) potential in mDC maturation [5]. The TICAM-1 pathway allows mDCs to activate IRF-1 and IRF-3, which in turn activate the IFN-β promoter as well as unidentified NK-driving factors. The data imply that the cross-priming and the NK-driving signals are also dependent upon TICAM-1, but the transcription factors utilized by TICAM-1 are wholly distinct from those of MyD88. We found that mDC TICAM-1-mediated NK activation largely relies on the IRF-3-derived NK-activating molecule (INAM) which promotes mDC-NK cell contact [6], in addition to the reported soluble mediators IL-15, IFN-α, and IL-12p70. Thus, the mode by which mDCs matured differs in the MyD88 and the TICAM-1 pathways. If an appropriate adjuvant is conjugated with vaccine, NK cells can be activated for eradication of microbes.

We have analyzed how mDCs acquire effector-driving functions by focusing on the innate immune response [1]. Live vaccines usually contain microbe-specific Ags and PAMPs. Since DNA *per se* has an adjuvancy, DNA vaccine also includes PAMPs. Nevertheless, potential vaccines have not been established for some viral infec-

* Corresponding author. Tel.: +81 11 706 5073; fax: +81 11 706 7866.
E-mail address: seya-tu@pop.med.hokudai.ac.jp.

0264-410X/$ – see front matter © 2010 Elsevier Ltd. All rights reserved.
doi:10.1016/j.vaccine.2010.09.023

tions. For example, HCV, HIV and influenza infections have their own problems. Low titers of antiviral antibody and CTL induction may be dissolved by developing efficient adjuvants which potentially augment appropriate effectors. In this stand, an effective strategy for tackling the issue of low immune response against vaccines has yet to be proposed with obstinacy infectious diseases. Even if the fundamental immune aberrance is present in the focal nests of infection. The microenvironmental situation should be grasped by researchers and be improved by their best. If this is feasible, adjuvant therapy be a good choice for some virus-induced persistent infections.

There is almost no information concerning the molecular mechanisms by which mDCs drive these effector cells. Each DC subset seems to correspond to a specific effector, although the selection strategy about how DCs induce various effectors is not clear in most instances. However, it is known from mouse models that splenic CD8+ DCs induce Treg [7] and NK cells [8] in the mouse spleen, and lamina propria pDCs in the mouse enteric canal promotes IgA production [9]. In addition, CD70+/CD11c+ DCs induce Th17 cells by the ATP of enterobacteria [10], and bone-marrow (BM)DCs markedly activate NK cells via the TICAM-1 pathway [11]. It is known that plasmacytoid dendritic cells (pDCs) induce tremendous amounts of IFN-α in response to CpG DNA through TLR9. Although what molecular background supports this pDC phenotype has long been unknown, pDC-specific events should regulate the activation of IRF-7 ([12], also see the review of T. Kaisho in this issue). Further examples of DC subsets that preferentially function with specific effectors will likely be demonstrated through continued investigation.

For future studies, it is necessary to determine the potential of peptide-conjugating materials including Ags and inflammation-inducing reagents. A number of reports have suggested that adjuvants can greatly increase the efficiency rate of treatment, although there are no criteria to fairly evaluate the function of adjuvants in vaccine recipients or patients. The method for stimulating DCs needs to be carefully selected as systemic administration of inflammation-inducing material can also lead to the acceleration or exacerbation of infection at the same time. In this case, the route and molecule that selectively raise the degree of DC maturation without severe malicious inflammation should be clarified. The design of DC maturation can be manipulated without helping flare inflammation. In the future, we hope that through continued research, patients will have access to convenient and highly effective prophylactic immunotherapy.

Acknowledgement

We are grateful to Dr. H. Kida (Hokkaido University, Sapporo) for his giving us this opportunity.

References

[1] Seya T, Shime H, Ebihara T, Matsumoto M. Pattern recognition receptors of innate immunity and their application to tumor immunotherapy. Cancer Sci 2010;101:313–20.
[2] Akira S, Uematsu S, Takeuchi O. Pathogen recognition and innate immunity. Cell 2006;124:783–801.
[3] Matumoto M, Seya T. TLR3: interferon induction by double-stranded RNA including poly(I:C). Adv Drug Deliv Rev 2008;60:805–12.
[4] Akazawa T, Masuda H, Saeki Y, Matsumoto M, Takeda K, Tsujimura K, et al. Adjuvant-mediated tumor regression and tumor-specific cytotoxic response are impaired in MyD88-deficient mice. Cancer Res 2004;64:757–64.
[5] Akazawa T, Ebihara T, Okuno M, Okuda Y, Shingai M, Tsujimura K, et al. NK activation induced by the Toll-like receptor 3-TICAM-1 (TRIF) pathway in myeloid dendritic cells. Proc Natl Acad Sci USA 2007;104:252–7.
[6] Ebihara T, Azuma M, Oshiumi H, Iwabuchi K, Taniguchi T, Matsumoto M, et al. Identification of INAM, a polyI:C-inducible membrane protein, that participates in dendritic cell-mediated natural killer cell activation. J Exp Med, in press.
[7] Yamazaki S, Dudziak D, Heidkamp GF, Fiorese C, Bonito AJ, Inaba K, et al. CD8+ CD205+ splenic dendritic cells are specialized to induce Foxp3+ regulatory T cells. J Immunol 2008;181:6923–33.
[8] Miyake T, Kumagai Y, Kato H, Guo Z, Matsushita K, Satoh T, et al. Poly I:C-induced activation of NK cells by CD8 alpha+ dendritic cells via the IPS-1 and TRIF-dependent pathways. J Immunol 2009;183:2522–8.
[9] Tezuka H, Abe Y, Iwata M, Takeuchi H, Ishikawa H, Matsushita M, et al. Regulation of IgA production by naturally occurring TNF/iNOS-producing dendritic cells. Nature 2007;448:929–33.
[10] Atarashi K, Nishimura J, Shima T, Umesaki Y, Yamamoto M, Onoue M, et al. ATP drives lamina propria T(H)17 cell differentiation. Nature 2008;455:808–12.
[11] Ebihara T, Shingai M, Matsumoto M, Wakita T, Seya T. Hepatitis C virus-infected hepatocytes extrinsically modulate dendritic cell maturation to activate T cells and natural killer cells. Hepatology 2008;48:48–58.
[12] Hoshino K, Sugiyama T, Matsumoto M, Tanaka T, Saito M, Hemmi H, et al. IkappaB kinase-alpha is critical for interferon-alpha production induced by Toll-like receptors 7 and 9. Nature 2006;440:949–53.

OPEN ACCESS Freely available online

PLoS one

The Peptide Sequence of Diacyl Lipopeptides Determines Dendritic Cell TLR2-Mediated NK Activation

Masahiro Azuma[1☯], Ryoko Sawahata[1☯], Yuusuke Akao[1☯¤a], Takashi Ebihara[1¤b], Sayuri Yamazaki[1], Misako Matsumoto[1], Masahito Hashimoto[2], Koichi Fukase[3], Yukari Fujimoto[3], Tsukasa Seya[1]*

1 Department of Microbiology and Immunology, Graduate School of Medicine, Hokkaido University, Sapporo, Japan, **2** Department of Nanostructure and Advanced Materials, Kagoshima University, Kagoshima, Japan, **3** Department of Chemistry, Graduate School of Science, Osaka University, Toyonaka, Japan

Abstract

Natural killer (NK) cells are lymphocyte effectors that are activated to control certain microbial infections and tumors. Many NK-activating and regulating receptors are involved in regulating NK cell function. In addition, activation of naïve NK cells is fundamentally triggered by cytokines or myeloid dendritic cells (mDC) in various modes. In this study, we synthesized 16 S-[2,3-bis(palmitoyl)propyl]cysteine (Pam2Cys) lipopeptides with sequences designed from lipoproteins of *Staphylococcus aureus*, and assessed their functional properties using mouse (C57BL/6) bone marrow-derived DC (BMDC) and NK cells. NK cell activation was evaluated by three criteria: IFN-γ production, up-regulation of NK activation markers and cytokines, and NK target (B16D8 cell) cytotoxicity. The diacylated lipopeptides acted as TLR2 ligands, inducing up-regulation of CD25/CD69/CD86, IL-6, and IL-12p40, which represent maturation of BMDC. Strikingly, the Pam2Cys lipopeptides induced mouse NK cell activation based on these criteria. Cell-cell contact by Pam2Cys peptide-stimulated BMDC and NK cells rather than soluble mediators released by stimulated BMDC induced activation of NK cells. For most lipopeptides, the BMDC TLR2/MyD88 pathway was responsible for driving NK activation, while some slightly induced direct activation of NK cells via the TLR2/MyD88 pathway in NK cells. The potential for NK activation was critically regulated by the peptide primary sequence. Hydrophobic or proline-containing sequences proximal to the N-terminal lipid moiety interfered with the ability of lipopeptides to induce BMDC-mediated NK activation. This mode of NK activation is distinctly different from that induced by polyI:C, which is closely associated with type I IFN-inducing pathways of BMDC. These results imply that the MyD88 pathway of BMDC governs an alternative NK-activating pathway in which the peptide sequence of TLR2-agonistic lipopeptides critically affects the potential for NK activation.

Citation: Azuma M, Sawahata R, Akao Y, Ebihara T, Yamazaki S, et al. (2010) The Peptide Sequence of Diacyl Lipopeptides Determines Dendritic Cell TLR2-Mediated NK Activation. PLoS ONE 5(9): e12550. doi:10.1371/journal.pone.0012550

Editor: Jacques Zimmer, Centre de Recherche Public de la Santé, Luxembourg

Received June 10, 2010; **Accepted** July 30, 2010; **Published** September 2, 2010

Funding: This work was supported in part by Grants-in-Aid from the Ministry of Education, Science, and Culture (Specified Project for Advanced Research) and the Ministry of Health, Labor, and Welfare of Japan, and by the Yakult and Waxmann Foundations. Financial support by the Sapporo Biocluster "Bio-S" the Knowledge Cluster Initiative of the MEXT, is gratefully acknowledged. The funders had no role in study design, data collection and analysis, decision to publish, or preparation of the manuscript.

Competing Interests: The authors have declared that no competing interests exist.

* E-mail: seya-tu@pop.med.hokudai.ac.jp

☯ These authors contributed equally to this work.

¤a Current address: Yakult Central Institute for Microbiological Research, Kunitachi, Tokyo, Japan
¤b Current address: Howard Hughes Medical Institute, Washington University School of Medicine, St. Louis, Missouri, United States of America

Introduction

Natural killer (NK) cells function in early defense against various pathogens. Microbial pattern molecules activate NK cells by stimulating pattern-recognition receptors (PRRs) in NK cells or myeloid dendritic cells (mDC) [1]. mDC-mediated NK activation occurs secondary to mDC maturation, and is competent to induce NK-activating cytokines or mDC membrane molecules to facilitate reciprocal activation of mDC and NK cells [1,2]. Toll-like receptors (TLRs) and cytoplasmic pattern sensors are PRRs that may be associated with mDC-mediated NK activation [1,3]. In mDC, TLR3 and cytoplasmic sensors, RIG-I/MDA5 usually participate in driving NK activation in response to double-stranded (ds)RNA [4–6].

Staphylococcus aureus, a versatile Gram-positive pathogen, is reported to activate NK cells during infection [7]. *S. aureus* cell wall components including peptidoglycan, lipoproteins, and alanylated lipoteichoic acid, are inflammation inducers, and provoke the activation of host immune cells [8]. *S. aureus* cell wall pattern molecules are mainly recognized by cell-surface TLR2 and cytoplasmic nucleotide-binding oligomerization domain 2 (Nod2) in host cells, which signal the presence of bacterial infection. Mice lacking TLR2 or the adaptor protein MyD88 are highly susceptible to *S. aureus* infection [9]. The molecular basis by which *S. aureus* activates host immunity has been investigated, and lipoprotein, rather than lipoteichoic acid, is the main trigger of immune stimulation [10] that preferentially activates TLR2 in mouse cells. TLR2/MyD88 determines the pathway for activation of macrophages in mice [11]. Lipoprotein also activates TLR2 in human cells [12,13].

The functional properties of *S. aureus* lipopeptides have been investigated in gene-disrupted mice [9,14,15]. TLR2, in concert with TLR1 or TLR6, is involved in their recognition [16,17]. Two adaptor proteins, TIRAP and MyD88, deliver TLR2 signals that